HHS Public Access

Author manuscript

Int J Radiat Oncol Biol Phys. Author manuscript; available in PMC 2022 August 18.

Published in final edited form as:

Int J Radiat Oncol Biol Phys. 2021 May 01; 110(1): 68–86. doi:10.1016/j.ijrobp.2020.08.013.

Single and Multi-fraction Stereotactic Radiosurgery Dose/Volume Tolerances of the Brain

Michael T. Milano, MD PhD[1], **Jimm Grimm, PhD**[2], **Andrzej Niemierko, PhD**[3], **Scott G. Soltys, MD**[4], **Vitali Moiseenko, PhD**[5], **Kristen J. Redmond, MD**[6], **Ellen Yorke, PhD**[7], **Arjun Sahgal, MD**[8], **Jinyu Xue, PhD**[9], **Anand Mahadevan, MD**[2], **Alexander Muacevic, MD**[10], **Lawrence B. Marks, MD**[11], **Lawrence R. Kleinberg, MD**[6]

[1]Department of Radiation Oncology, University of Rochester, 601 Elmwood Ave. Box 647, Rochester, NY.

[2]Department of Radiation Oncology, Geisinger Cancer Institute, Danville, PA.

[3]Department of Radiation Oncology, Massachusetts General Hospital, Boston, Massachusetts

[4]Department of Radiation Oncology, Stanford University Medical Center, 875 Blake Wilbur Dr, Stanford, CA

[5]Department of Radiation Medicine and Applied Sciences, University of California San Diego, La Jolla, CA.

[6]Department of Radiation Oncology & Molecular Radiation Sciences, Johns Hopkins University School of Medicine, Baltimore, MD

Corresponding Author: Michael T. Milano, Department of Radiation Oncology, University of Rochester, Rochester, NY 14642. Phone: 585-273-4096, Fax: 585-275-1531, michael_milano@urmc.rochester.edu.

Conflict of Interest:

MTM: Dr. Milano reports Royalties from UpToDate, and royalties from Galera Therapeutics outside the submitted work.

JG: Dr. Grimm reports grants from Accuray, grants from NovoCure, outside the submitted work; In addition, Dr. Grimm has a patent DVH Evaluator issued.

AN: none

SGS: Dr. Soltys reports personal fees from Inovio Pharmaceuticals, Inc., personal fees from Zap Surgical, Inc., grants from Novocure, outside the submitted work.

VM: None

KJR: Dr. Redmond reports grants and other from Elekta AB, grants and other from Accuray, personal fees from BioMimetix, other from Brainlab, outside the submitted work.

EY: partly supported by NCI Cancer Center Support Grant P30CA008748

JX: None

AS: Dr. Arjun Sahgal has been an advisor/consultant with Abbvie, Merck, Roche, Varian (Medical Advisory Group) and Elekta (Gamma Knife Icon); ex officio Board Member to International Stereotactic Radiosurgery Society (ISRS); received honorarium for past educational seminars with Elekta AB, Accuray Inc, Varian (CNS Teaching Faculty), BrainLAB and Medtronic Kyphon; research grant with Elekta AB; and travel accommodations/expenses by Elekta, Varian and BrainLAB. Dr. Sahgal also belongs to the Elekta MR Linac Research Consortium, Elekta Spine, Oligometastases and LINAC Based SRS Consortia.

AM: Dr. Mahadevan reports personal fees from Varian Inc, non-financial support from Accuray Inc, outside the submitted work

AM: Dr. Muacevic receives speaker honoraria from Accuray Inc. and was former president and chairman of The Radiosurgery Society, therss.org.

LBM: none

LRK: Dr. Kleinberg reports grants, personal fees and other from Novocure, grants and personal fees from Accuray, grants from Arbor, outside the submitted work

[7]Department of Medical Physics, Memorial Sloan–Kettering Cancer Center, New York, NY

[8]Department of Radiation Oncology, Odette Cancer Centre, Sunnybrook Health Sciences Centre, University of Toronto, Toronto, ON, Canada

[9]Department of Radiation Oncology, NYU Langone Medical Center, New York, NY 10016

[10]European Cyberknife Center Munich-Großhadern, Munich, Germany

[11]Department of Radiation Oncology and Lineberger Cancer Center, University of North Carolina, Chapel Hill, NC

Abstract

Purpose/Objective(s)—As part of the American Association of Physicists in Medicine (AAPM) Working Group on Stereotactic Body Radiotherapy, investigating normal tissue complication probability (NTCP) after hypofractionated radiotherapy, data from published reports (PubMed indexed 1995–2018) were pooled to identify dosimetric and clinical predictors of radiation-induced brain toxicity after single-fraction stereotactic radiosurgery (SRS) or fractionated stereotactic radiosurgery (fSRS).

Materials/Methods—Eligible studies provided normal tissue complication probabilities (NTCPs) for the endpoints of radionecrosis, edema, or symptoms after cranial SRS/fSRS, and quantitative dose-volume metrics. Studies of patients with only glioma, meningioma, vestibular schwannoma, or brainstem targets were excluded. The data summary and analyses focused on arteriovenous malformations (AVM) and brain metastases.

Results—Data from 51 reports are summarized. There was wide variability in reported rates of radionecrosis. Available data for SRS/fSRS for brain metastases were more amenable to NTCP modeling than AVM data. In the setting of brain metastases, SRS/fSRS-associated RN can be difficult to differentiate from tumor progression. For single-fraction SRS to brain metastases, volumes receiving 12 Gy (V12), including the target volumes, of 5 cc, 10 cc, or >15 cc were associated with risks of symptomatic radionecrosis of approximately 10%, 15%, and 20%, respectively. SRS for AVM was associated with modestly lower rates of symptomatic radionecrosis for equivalent V12. For 3-fraction fSRS for brain metastases, normal brain tissue V18 <30 cc and V23 <7 cc were associated with <10% risk of radionecrosis.

Conclusions—The risk of radionecrosis after SRS and fSRS can be modeled as a function of dose and volume treated. The use of fSRS appears to reduce risks of radionecrosis for larger treatment volumes relative to SRS. More standardized dosimetric and toxicity reporting is needed to facilitate future pooled analyses that can refine predictive models of brain toxicity risks.

SUMMARY:

Pooled published data reveal that radiation-induced brain toxicity after single fraction stereotactic radiosurgery (SRS) for brain metastases and arteriovenous malformations is low when the volume of tissue receiving 12 Gy is less than 5 cc but increases with larger treatment volumes. Fractionated SRS can reduce toxicity risk for larger targets. Standardized dosimetric and toxicity reporting would facilitate future pooled analyses and predict brain toxicity risks more precisely.

1. CLINICAL SIGNIFICANCE

Single-fraction radiosurgery (SRS) or hypofractionated (2–5 fraction) cranial radiosurgery (fSRS) are commonly used for various primary and metastatic brain tumors. Radiation-induced necrosis (radionecrosis), edema and other neurologic complications are relatively common. Radiation necrosis represents inflammation from tissue death and breakdown, and is generally associated with surrounding edema, which can be either symptomatic or asymptomatic. Although terminology in the literature varies, and includes necrosis, radionecrosis, radiation treatment effect, treatment-related imaging changes and adverse radiation effect (ARE, including reactive inflammation, vasculitis, and necrosis) [1], herein the terms necrosis, radionecrosis and radiation necrosis are used (unless specifying the outcome used in a specific report). In most studies, the onset of necrosis ranges from <6 months to several years after SRS/fSRS, with median time to onset of roughly a year.

Symptomatic necrosis can result from direct brain injury, or from necrosis within the target that elicits an inflammatory cascade [1], that can cause mass effect and/or surrounding edema with associated compression (and at the extreme, herniation) of normal brain. Necrosis is thought to be mediated via vascular endothelial injury [1–3]. Edema in the absence of necrosis can also occur. Symptoms of edema and/or necrosis include headache, nausea, vomiting, ataxia, seizure, and focal site-dependent functional deficits.

Asymptomatic necrosis can be managed with clinical and radiographic surveillance. For symptomatic necrosis, corticosteroids are considered first-line therapy [4,5], with the dose, schedule and duration of corticosteroids dependent upon the response of symptoms and possible complications of their treatment (e.g., myopathy with motor weakness, osteopenia, hypertension, extremity edema, obesity with accumulation of subcutaneous fat, and glucose intolerance) [4]. Emerging data have shown favorable radiographic and clinical responses of brain radionecrosis to bevacizumab [6,7]; in addition, bevacizumab may reduce the need for corticosteroids. A small (n=14) randomized double-blind, placebo-controlled study, allowing for cross over to the treatment arm, provided compelling evidence of the efficacy bevacizumab for brain radionecrosis [8], though bevacizumab was associated with relatively high risks (in 3 of 11 patients) of severe toxicity (aspiration pneumonia, pulmonary embolus and superior sagittal sinus thrombosis), warranting caution before considering this therapy. An Alliance study had planned to randomize 130 patients *(currently closed after accrual of 18)* with symptomatic post-SRS brain radionecrosis to corticosteroids with or without bevacizumab; the primary endpoint was patient-reported outcome (symptoms) of radionecrosis, and the study allowed cross over to the treatment arm (NCT02490878). Hyperbaric-oxygen therapy may have some efficacy against brain radionecrosis, though this treatment remains investigational [4,5]. Radionecrosis that is resistant to medical management can be considered for surgical resection or laser-interstitial thermal therapy (LITT) with biopsy, which are often considered when persistent/recurrent tumor is in the differential diagnosis.

2. ENDPOINTS

The common brain toxicity endpoints reported in the literature include necrosis, edema, and neurologic compromise. Radionecrosis is often evident as a ring-enhancing lesion, commonly with associated edema.

For tumors, SRS/fSRS-associated radionecrosis can be difficult to differentiate from tumor progression or pseudo-progression. Necrosis can be symptomatic or asymptomatic, and the diagnosis can be made based upon imaging findings or pathologic confirmation (which may reveal a mixture of necrosis and viable tumor). Pathologic correlates with imaging findings are not commonly reported in studies of radionecrosis incidence. Most often the diagnosis is made based solely upon imaging findings. Techniques such as positron emission tomography, magnetic resonance (MR) cerebral perfusion, delayed-contrast MR imaging and MR spectroscopy, may help strengthen the diagnostic certainty [2,3,5,9]. The sensitivity and specificity of various imaging modalities used in differentiating between radionecrosis and tumor recurrence were recently summarized [4]. Overall, the sensitivity is on the order of 60–80% for most of these modalities in differentiating necrosis from tumor progression, and thus no single test can reliably distinguish radionecrosis from recurrent tumor, potentially requiring a multi-modal approach for some patients. Radiomic strategies, such as changes in MR imaging features, are also being investigated as a means to distinguish radionecrosis from tumor progression [10–12]. The lack of a consistent means to diagnose necrosis [13] complicates the interpretation of the data. Recognizing this challenge, the 2015 Response Assessment in Neuro-Oncology Brain Metastases (RANO-BM) working group report suggested that if lesion growth meets criteria for progression (“at least a 20% increase in the sum longest diameter of CNS target lesions,” relative to smaller of baseline or nadir, sustained for ≥4 weeks), but clinical evidence suggests treatment effect, additional evidence (not specified in the report) is needed to distinguish progression from treatment effect [14]. Thus, it is sometimes challenging to diagnose necrosis with confidence. The imaging manifestations in patients on immune therapies appear to be particularly challenging with respect to edema and necrosis versus immune response and, as a consequence, newer imaging criteria such as immunotherapy response assessment in neuro-oncology (iRANO) is being implemented [15].

Necrosis may cause a variety of different symptoms, and toxicity grading traditionally has been based on the *severity* of these symptoms (rather than can the extent/severity of the necrosis itself, for which there is no widely accepted grading scale). Several examples [16–18] are shown in Table 1. A more-detailed toxicity grading system specifically considered symptomatic, objective, management and analytic (SOMA) criteria [2,19], and while this approach has clear benefits for brain toxicity, it has not been widely adopted.

The most accurate means to diagnose radionecrosis is pathological confirmation. If surgery is required because of necrosis, then historically the necrosis was considered at least grade 3; although it is conceivable that some patients with no symptoms, or grade 1–2 symptoms, could undergo a planned resection to establish a diagnosis of recurrence vs. necrosis, and the pathologic findings be most consistent with necrosis. Therefore, an endpoint defined simply as “pathological confirmation of necrosis” may include lower grade events, potentially

overestimating the incidence of clinically significant necrosis. Nevertheless, grade 1–2 symptoms typically do not warrant a biopsy or surgery; and thus the determination of necrosis is less accurate in these patients. The more serious complications, that more often lead to biopsy or surgery, are based upon the more reliable pathological (versus clinical) assessment of necrosis.

3. CHALLENGES DEFINING VOLUMES

Defining the major structures of central nervous system is straightforward, although there is no consensus on how to delineate the sub-regions of the brain [20]. Auto-contouring software may erroneously include portions of the cavernous sinus, venous sinuses, or surgical deficits in the skull (i.e. post-craniotomy) as normal brain; we recommend excluding these regions, as well as cranial nerves and brainstem, from the brain organ at risk (OAR).

In published reports on necrosis risks after SRS/fSRS, there is variability in what volumes are used to correlate dose-volume exposure with toxicity risks. Specific volumes described (Supplemental Tables) include: 1) all tissue (i.e. all of the volume encompassed by isodose line, which includes target volume), 2) ‘normal’ or ‘non-target’ tissue, and 3) ‘surrounding brain’ or brain. For ‘brain’ or ‘surrounding brain’ tissue, there is some variability in what target volume (i.e. gross target, clinical target or planning target volumes) is subtracted from brain. Such variability complicates pooling of data. The differences in calculated volume exposures between these approaches would depend on the size of the target, location of the target, as well as the planning approaches used. As an example, assume a simple scenario of 2 spherical target volumes, surrounded by brain parenchyma, in which the 12 Gy isodose line is 3 mm from the target surface (not accounting for sharper dose-falloffs with smaller targets [21]). For a 0.4 cm target (0.034 cc), the brain V12 (0.49 cc) is similar to tissue V12 (0.52 cc). For a 2.5 cm target (8.2 cc), brain V12 (7.4 cc) is less than half of tissue V12 (15.6 cc). With a 2.5 cm spherical target (tissue V12 of 14.1 cc) abutting the brain surface, with 30% of the 12 Gy volume outside of brain, the brain V12 (5.2 cc) would be ~1/3 of tissue V12. From the models in Figures 1–6, it can be seen that in the flat regions a change of 1 cc in brain volume has less than 1% effect on risk, but in the steepest dose/volume response regions, a 5% change in risk could result from about 1 cc of volume uncertainty.

4. REVIEW OF OUTCOMES DATA

Published studies

PubMed searches were performed for reports published from January 1995 through December 2016 (including studies in print in 2017 that were published and indexed online in 2016); search criteria are detailed in the Supplemental Appendix. One additional study from 2018 was also included [22]. All of the searches included the word “volume” or “volumes.” Studies included in this review (listed in Supplemental Table 1) reported endpoints of symptomatic and/or asymptomatic necrosis and/or edema after SRS/fSRS, and correlated toxicity risks with target, tissue and/or brain volume or dose-volume metrics. We also included studies that used more generalized endpoints of radiation-induced neurologic (non-cranial nerve) complications (which generally comprise necrosis and/or edema). Those

studies that analyzed only potential effects of prescribed dose on toxicity risks (i.e. no analyses of target volume or normal tissue volume exposure) were not included in the Supplemental Tables or analyses (though some are discussed below), as the manner in which dose is prescribed is highly variable and does not necessarily reflect normal tissue dose-volume exposure. Target volumes also do not sufficiently describe normal tissue dose-volume exposure, but studies that analyzed target volume without analyzing normal tissue exposure were included here, as target volume is a reproducible measure. Studies of central nervous system radiotoxicity after conventionally-fractionated or >5-fraction hypofractionated stereotactic radiotherapy were omitted (unless a subset of 1–5 fraction SRS/fSRS patients was analyzed separately).

We excluded studies reporting toxicity outcomes in a cohort comprised solely of: 1) brainstem targets, as the brainstem appears to have a different dose tolerance than normal brain (see Section 7); 2) patients with glioma, as many gliomas have tumor-related necrosis prior to SRS/fSRS; 3) patients with vestibular schwannoma/acoustic neuroma, as these tumors are not within the brain parenchyma, intra-tumoral necrosis after SRS/fSRS is fairly common for vestibular schwannoma/acoustic neuroma, and neurologic radiotoxicity from these tumors is mostly related to cranial nerve, cochlear and/or brainstem injury; and 4) patients with edema after SRS/fSRS for meningioma, as the etiology of post-radiation edema may be unique for meningiomas [23]. Nevertheless, some of the studies included in this review did include a subset of patients with glioma, meningioma, vestibular schwannoma, or brainstem targets, but generally these represented a small subset of patients/tumors in these studies (specified in Supplemental Table 1), and these patients were not included in the pooled analyses specific for brain metastases and arteriovenous malformations (AVM).

Supplemental Table 1 summarizes 51 published reports, from which 9,828 patients and 13,913 targets were studied. Some reports [24–32] included a number of patients that were analyzed in one or more earlier reports. With estimation (due to partial overlap of some patients in multiple studies, as described in Supplemental Table 1) these reports considered approximately 7,814 unique patients. Most patients were treated for AVM or brain metastases: an estimated 3,848 patients had 3,858 AVMs, and 3,966 patients had 7,903 brain metastases. Most of these studies/patients were not amenable to modelling analyses but are included in the discussion and Supplemental Tables as they offered insight into NTCP risks.

Some studies included only patients with arteriovenous malformations (AVM) [24,25,31–40], others included only patients with benign and/or malignant tumors [26–30,41–70], and 4 others included patients with tumors or AVMs [71–74] (of which 3 analyzed the different disease groups separately). In 10 studies, some [30,50] or all [28,49,51,56,63,67,69,70] of the patients underwent SRS/fSRS to the surgical cavity of a resected brain metastasis.

Various endpoints (Supplemental Table 2) and dosimetric measures (Supplemental Tables 3–5) were used to characterize toxicity risks. For example, where Vx reflects the volume receiving greater than or equal to a dose of x Gy, several studies analyzed tissue Vx (i.e., volume of x Gy isodose line), others analyzed normal tissue Vx (i.e., excluding target

volume) and others analyzed brain Vx (i.e., excluding target volume and non-brain normal tissue). Endpoints in different studies included symptomatic brain necrosis (with some studies specifying toxicity grade), any necrosis, edema, neurologic complications (without specifying from necrosis or edema) and others (Supplemental Table 2). Such variability complicates data pooling.

A few studies reported only p values for the correlation of risks with dosimetric parameters, but not the risks within subgroups; therefore data from these studies did not allow binning subsets into groups for modelling. Supplemental Table 2 also summarizes the reported timing of the onset of necrosis, which in most studies ranges from <6 months to several years after SRS/fSRS, with median time to onset of roughly a year. Actuarial risks are only reported in some studies; therefore, our graphs that summarize published data (Figures 1–4 below) and NTCP models (section 6 and Figures 5–6) use crude toxicity risks.

For the datasets presented in Figures 1–4 (this section), with the data binned into subgroups of Vx (i.e., by quartiles or median splits), the logarithmic form of the logistic model (described in section 6) was used (Eq. 1).

$$NTCP = \frac{1}{1 + \left(\frac{Vx_{50}}{Vx}\right)^{4\gamma_{50}}} \quad (1)$$

Arteriovenous malformations

For AVMs, the concept of high dose volume exposure with SRS correlating with toxicity risks was recognized in the 1970s-1980s [75,76]. Flickinger and colleagues published several studies in the 1980s-1990s analyzing the relationship between necrosis/toxicity risks and dose-volume exposure in the treatment of tumors and AVMs [77–80]. The AVM Study Group described the effects of AVM location and tissue volume (including target) receiving ≥12 Gy (V12) in 1 fraction in predicting permanent sequelae [25]. Studies from several institutions have also demonstrated the importance of V10–12 in predicting toxicity risks of AVM patients [24,31,34,37–40,71]. Most studies of AVMs analyzed tissue V10–12 (i.e. included the target volume, as opposed to a V10–12 which excludes the target), which seems logical as the AVM interdigitates with brain tissue. In the AVM Study Group report, non-target V12 did not significantly improve the risk-prediction model; both target and non-target V8–12 were significant predictors of toxicity in another study [38].

Figures 1 and 2 show the reported risks of any or symptomatic necrosis after single-fraction SRS for AVM, relative to tissue V12, in those studies which grouped/binned patients/lesions by V10-V12. The combined factors of converting V10 in the Voges et al. study [31] to V12 (using Eq. 2 in section 6), and estimating the median values of V12 (see figure captions), produce uncertainties in the data compilation. Logistic models are shown merely as a descriptive way to summarize the data (and not intended to be predictive). For these logistic models, the logarithm of Vx (as opposed to Vx) was used for the independent variable (Eq. 1), to avoid predictions of a non-zero probability of necrosis for Vx=0; for the plots in Figures 1–2, the inverse log of that independent variable was used (to recreate ‘Vx’).

Target volume is also predictive of toxicity risks in AVM patients [31,35,36,38–40,71]. With AVMs, the reported rate of radionecrosis ranges from ~0–20% for small lesions and ~15–40% for lesions >10 cc; similar event rates are seen with low V12 vs. V12>10 cc, with variability between reports likely partially attributable to differences in analyzed endpoints (Supplemental Tables 3–5). In a multi-institutional study of 2,236 AVM patients with target volumes ranging from 0.1–24 (median 3) cc, multivariate analyses demonstrated that doses >24 Gy to the target margin, vs. lower doses, significantly (p=0.004) predicted a >1.5-fold risk of radiation-induced changes; no dose-volume metrics were analyzed [81].

Tumors

Among 135 patients with AVMs, benign skull base tumors and other benign tumors, Voges and colleagues reported risks of radiation-induced radiographic changes of 24% vs. 0% for V10>10 cc vs. ≤10 cc ($p<0.0001$), respectively. This study is a landmark publication, being among the first to correlate toxicity risks with SRS dose-volume metrics for tumors [71]. Two other early (2001) studies, that grouped together benign intracranial tumors, gliomas, brain metastases and AVMs in their analyses, evaluated SRS dose-volume metrics associated with necrosis and complication risks [72,73]. Chin et al. compared the dosimetry in 17 patients who developed symptomatic necrosis vs. 17 controls who did not, and reported that total-volume V10 (median 28.4 vs. 7.8 cc, p=0.007), brain V10 (19.8 vs. 7.1 cc, p=0.005) and target volume (4.4 vs. 1.5 cc, p=0.04) were significantly greater in the necrosis group [73]. Nakamura et al. reported that, among 657 evaluable patients with 1,244 targets, prescription volume (p=0.009), target volume (p=0.007) and non-target volume (p=0.03) correlated with grade 3 complications risks [72]; prescription volumes of ≤0.66 cc, 0.67–3.0 cc, 3.1–8.6 cc, and ≥8.7 cc were associated with grade 3 complication rates of 0%, 3%, 7% and 9%.

Brain metastases

For metastatic malignant brain tumors, earlier studies on toxicity risks focused on peripheral dose and tumor size. The RTOG 90–05 phase I study (which included recurrent, previously irradiated brain metastases and gliomas) reported 2-year actuarial neurotoxicity risks of 11% [82]. With lesions grouped by maximum diameter, crude rates of grade ≥3 neurotoxicity were 10% for ≤2.0 cm lesions treated to peripheral dose of 24 Gy, 20% for 2.1–3.0 cm lesions treated to 18 Gy and 14% for lesions 3.1–4.0 cm treated to 15 Gy. In multivariate analyses, tumor diameter was associated with significantly increased risk of grade ≥3 neurotoxicity, with 7.3 and 16-fold increased risks for tumors 2.1–3.0 and 3.1–4.0 cm (respectively) versus in tumors ≤2.0 cm. A 2017 study from Cleveland Clinic [83], with 896 patients with 3,034 brain metastases ≤2 cm, showed that tumor diameter >1 cm (vs. <1 cm) was associated (on multivariate analysis) with a 2.1-fold increased risk of necrosis, and 4.8-fold increased risk of symptomatic necrosis; similar risks (on univariate analyses) were seen with tumor volume >0.1 cc. Another study reported that maximum dose divided by lesion diameter was predictive of grade 3–4 necrosis risks [84].

For smaller lesions that might be safely treated to relatively high doses, clinicians generally opt against exceeding a prescribed dose of 24 Gy. A University of Kentucky study of patients with brain metastases ≤2.0 cm in size reported non-significantly greater grade 3–

4 toxicity rates (5.9% vs. 1.9%, p=0.078) with peripheral SRS doses >20 Gy (vs. lower doses) following whole brain radiotherapy (WBRT) [85]. This finding may not be applicable for patients treated with SRS alone (i.e., no WBRT). A prescribed dose of >17 Gy was predictive of any (asymptomatic or symptomatic) necrosis (HR 3.3, p=0.03) in another study [68]. In the aforementioned study from Cleveland Clinic (including lesions ≤2 cm) [83], dose >24 Gy was not associated with increased necrosis risks.

Target volume correlates with toxicity risks in many studies. The University of Pittsburgh described risks of neurologic complications of 3% versus 16% at 5-years for target volume ≤2 cc vs >2 cc (p=0.0085) [41]. These findings are comparable to other reports [29,52,53,72] (Supplemental Tables 3–5), two of which converted 3–5 fraction fSRS to single-fraction equivalent dose [52,53]. In two studies, tumor volume did not predict risk of neurologic complications [42,45]. In a BC Cancer Agency study, of brain metastases <3 cm in size, the reported necrosis risks were relatively high compared to other studies; for lesions greater vs. less than 0.4 cc, necrosis rates were 12% vs. 6% [61].

Beginning in the early 2000s, several studies described dose-volume measures predictive of radionecrosis, edema and neurologic complications after SRS/fSRS for brain metastases. The University of California San Francisco (UCSF) published one of the largest studies of brain metastases patients, in which the 1-year risks of symptomatic ARE were 1%, 6% and 13% for tissue V12 of ≤1.84 cc, 1.86–3.30 cc, and >3.3 cc respectively [29]. In a University of Cincinnati study [46], necrosis (asymptomatic or symptomatic) risks were 4.7% and 11.9% for V12 <1.6 cc and 1.6–4.7 respectively, comparable to the UCSF study. A much higher toxicity rate was reported in a Case Western Reserve study, with 23% of brain metastases with V12<5 cc developing symptomatic necrosis and 15% developing asymptomatic necrosis [43]. With V12 in excess of 10 cc, necrosis rates were >50% in the University of Cincinnati and Case Western Reserve studies [43,46], and lower in the USCF study [29] where a 15% necrosis rate (11% symptomatic) was reported with V12 of 7–35 cc. A study by Minniti and colleagues analyzed brain V12 (as opposed to tissue V12), showing a similar trend of increased V12 associated with increased toxicity risks, and similarly high rate (~50%) of toxicity with V12 >10 ml [47]. In Minniti and colleagues' 2016 study of 151 patients with brain metastases >2 cm [65], brain V12 remained significant (p=0.02) for radionecrosis risks, with a V12 >18.2 cc associated with a ~50% risk of radionecrosis.

Several studies (n=15, dating back to 2006 in the Supplemental Tables) have reported neurotoxicity risks after fSRS. Patients selected for fSRS often have bulkier disease and/or tumors in critical locations. Toxicity after fSRS appears to be favorable (Supplemental Tables 3–5), with recent meta-analyses suggesting that tumor control is not compromised, relative to single-fraction SRS, with the current dose-fractionation schedules commonly used [86,87]. Minniti and colleagues examined V15–24 with a 3-fraction schedule for patients with intact [54] or resected [49] brain metastases; <25 cc of normal brain receiving >18 Gy [54] and <17 cc receiving >24 Gy [49] were associated with <5% necrosis risks [49,54]. In Minniti and colleagues' 2016 study of 138 patients with brain metastases >2 cm treated to a dose of 9 Gy x 3 [65], a brain V18 of 22.8–30.2 cc, 30.2–41.2 cc and >41.2 cc was associated with 6%, 13% and 25% radionecrosis risks respectively. In studies from Inoue and colleagues [52,53], non-target V23.1 (3 fractions) <5 cc and <7 cc were

associated with 1.4% and 0% risks of symptomatic edema and necrosis requiring surgery, respectively; and V28.8 (5 fractions) <3 cc and <7 cc were associated with 0% risks of symptomatic edema and necrosis requiring surgery, respectively. A V23.1 in 3 fractions and V28.8 in 5 fractions were considered dose-equivalent to 14 Gy in 1 fraction (using an alpha-beta ratio of 2 Gy). Escalating prescribed dose from 9 to 10 Gy x 3 for brain metastases >3 cm increased the risks of radionecrosis, without apparent improvement in tumor control, in a recent dose-escalation study [88]. In a 2017 study of 2-fraction SRS [89], published after our 2016 cut-off, brain V20–87.8 values were analyzed as factors potentially associated with necrosis risks (albeit with only 4 events in 39 patients), with significant p values at V44.5-87.8.

The reported risks of any necrosis (Figure 3) and symptomatic necrosis (Figure 4) after SRS or fSRS for brain metastases, relative to tissue or brain V12 in a single-fraction dose equivalent, are shown for those studies that reported necrosis risks and median Vx among all patients/lesions, or grouped/binned patients/lesions by tissue or brain Vx. As with Figures 1–2 (see above) the logarithm of Vx was used for risk calculation in the model, to avoid predictions of a non-zero probability of necrosis for Vx=0.

A 2020 analysis (published after our literature search) of 5-fraction fSRS for intact brain metastases (n=132) reported that a brain (minus CTV) V30 of <10.5 cc vs. ≥10.5 cc was associated with a significantly greater risk of symptomatic ARE (13% vs. 61%), with a >7 fold relative-risk on multivariable analysis [90]. The 61% risk is appreciably higher than what is reported in most fSRS series (Figure 4), though few lesions in these other studies had many patients with brain (minus CTV) V30 >10.5 cc.

An issue specific to multi-target fSRS/SRS (a common situation with brain metastases) is whether Vx is reported per lesion or per patient (i.e., from the composite plan), and whether risks of necrosis are reported per lesion or per patient. In a 2020 study of single-fraction SRS in 40 patients with ≥10 brain metastases, the V12 of individual targets predicted risks of post-treatment changes suggestive of necrosis, as opposed to the net V12 [91]. Of the studies shown in Figures 3–4, one [44] analyzed composite Vx and necrosis risks per patient, two [54,65] analyzed necrosis risks per patient, grouped by lesion (generally the largest) Vx (*personal communication, G. Minniti*), two [49,70] included patients with 1 or ~1 target (resected brain metastasis) per patient, and all of the others analyzed Vx and necrosis risks per lesion. All of the studies in Figure 3B reported necrosis risks per patient (including the 2 studies of SRS/fSRS for resection cavities and 2 studies that analyzed lesion Vx); all of the studies in Figure 4 reported necrosis risks and Vx per lesion. The logistic models of the data demonstrated significantly greater risks after SRS vs. fSRS, for both any necrosis (Figure 3, p<0.0001) and symptomatic necrosis (Figure 4, p<0.0001), with the caveat that for symptomatic necrosis (Figure 4) the endpoint in all of the fSRS studies was *symptomatic necrosis requiring surgical resection* versus the less stringent endpoint of *any symptomatic necrosis* that what was used in the SRS studies.

For any given value of Vx, the Vx for *tissue* exposure should represent *less* irradiated normal brain than the Vx for *brain* (since the *tissue* includes both normal brain and other tissues), and thus the risk of toxicity should be less *for tissue vs brain* (at the same Vx). As

shown in Figures 3 and 4, this is expected finding is not seen in the reported clinical data (perhaps reflecting heterogeneity in study populations and reporting methods/standards, and the challenges comparing data across institutions). In Supplemental Figures S1–3, risks of necrosis are plotted against tissue V12 (similarly to Figures 3–4), with tissue V12 estimated (for those studies that reported brain V12), by adding the brain V12 to the estimated target volume (which considered the range and median target volumes that were reported in the studies). As anticipated, the risk of necrosis relative to estimated V12 was lower using this method.

The combined factors of variable use of brain vs. tissue Vx, variable use of patient vs. lesion Vx, variable reporting of toxicity risks per patient vs. per lesion, conversion of single-fraction V10 or V14 to V12, conversion of multi-fraction fSRS Vx to single-fraction equivalent V12, and estimating median values of V12 (see Eq. 2 in section 6 and figure captions), produce uncertainties in the data compilation. Therefore, the logistic models should be considered as a descriptive way to summarize the data (and are not intended to be predictive).

5. FACTORS AFFECTING OUTCOMES

Radionecrosis, edema and neurotoxicity are multifactorial, with risks attributable to dose and volume (and perhaps surface area), and also likely related to target type (i.e. malignant tumor, benign tumor, AVM), target location, prior radiotherapy, prior surgery, systemic therapy, comorbid conditions, etc. Radiation toxicity likely represents injury to cells within the target and/or surrounding normal brain tissue [3,92]. Supplemental Table 6 summarizes variables, other than target volume and Vx, that were or were not significantly correlated with toxicity risks in each study. For any given variable, there was inconsistency across various studies. Nevertheless, there are some broad patterns.

In general, sex was not a significant risk factor; specifically, female sex was implicated as a risk factor in only 1 study [28]. Age was not a significant factor in most studies; in only 2 studies was older age an adverse risk factor [28,36]. CNS target location appears to be associated with toxicity risk, with more eloquent brain areas (such as thalamus, basal ganglia, occipital lobes) generally being more susceptible to symptomatic toxicity [24,25,30,32–34,36,37,43,45,47,48,60,61,74]; albeit with location being defined somewhat inconsistently. Conformity index/conformality was a significant factor in some studies [30,47,48,72] and not others [42,43,49,54,55]; counter-intuitively, lower conformity index (i.e., greater conformality) was associated with increased risk in one study [72], perhaps a spurious finding. Among patients with brain metastases, prior WBRT was generally not a significant factor for toxicity risk [29,41,46,48,55,69,73,83], though was implicated in some studies [43,60,69].

The potential impact of histology of brain metastases remains unclear. In 3 studies [42,59,70], cancer type was not a significant variable. However, several other studies reported different findings (though it remains unclear if the associations of some cancer types with greater risks of necrosis in these studies are from inherent differences between cancers, or differences in systemic therapy used). Kidney cancer (n=47 of 316 lesions) was

associated with a 2.4 fold risk of severe neurologic complications in one study [45]. In another study of 435 patients (2,200 lesions), kidney cancer (n=26 patients with 86 lesions) was associated with increased risk of adverse events among patients with tumors >1 cc [29]. In a 2016 study from the University of Maryland [62], renal or melanoma (n=24 patients) vs. lung or breast (n=83 patients) histologies were associated with a >2-fold greater risk of acute (within 100 days) edema. In a 2016 study from the Cleveland Clinic, among 1,939 patients with 5,747 lesions, renal cancer (HR 1.78, p=0.03) was associated with increased risks of radionecrosis after SRS; among NSCLC patients (2,276 lesions) adenocarcinoma histology (HR 1.89, p=0.04) and ALK rearrangement (HR 6.36, p<0.01) were also associated with radionecrosis [93].

In patients having both surgery and SRS/fSRS, symptomatic necrosis has been reported to be more common with post- vs. pre-resection SRS/fSRS (2 years: 17% vs 3% at 2 years; p=0.01) [30]. In a 2017 analysis, restricted to lesions ≥2 cm diameter (≥ ≈4 cc volume), the 1-year necrosis rates following post-operative SRS, pre-operative SRS and SRS alone were 23% vs 5% and 12%, respectively (p<0.001) [94].

6. MATHEMATICAL/BIOLOGICAL MODELS

At the time of the literature search, there were four articles that presented SRS/fSRS dose (in 1–5 fractions), target volume and toxicity outcome per treated target; an additional article with this level of granularity of data has recently been published. Data from these 5 studies, summarized in Table 2, were amenable to NTCP modelling. These studies included mostly patients with brain metastases, though 2 studies also included patients with glioma and benign tumors. We did not similarly model necrosis risks after SRS/fSRS for AVMs, as the published data did not lend itself to NTCP modelling.

The two earliest datasets that were used in our models were from studies of patients who underwent single-fraction SRS with Gamma Knife [43,73]. The 3 other studies included patients treated with single- and/or multi-fraction SRS; the doses from these datasets were converted to single-fraction equivalent doses, using the linear quadratic (LQ) model with α/β=2 Gy [22,52,53]. To form a composite model in terms of V12Gy (a commonly used dose metric for brain SRS), a simple ratio was used to approximate V12Gy from V10Gy and V14Gy [95,96]:

$$\begin{aligned} V12Gy &\approx V14Gy*(1+Delta) \\ V12Gy &\approx V10Gy/(1+Delta) \end{aligned} \tag{2}$$

The average Delta=0.5 was measured from the V10Gy, V12Gy, and V14Gy values in the appendix of Peng et al. [22]. The impact of elapsed treatment time is not considered in these calculations.

In the articles by Inoue et al. [52,53], GTV was subtracted from the brain contours to calculate brain Vx. Prior to modeling, we added the median GTV to brain Vx to approximate tissue Vx. Combined data from the studies listed in Table 2 were fit to a logistic

model [97] to generate curves describing probability of toxicity as function of V12Gy and V14Gy.

For the datasets presented in Figures 5–6 (this section), using studies that provided individual patient/lesion data, the exponential form of the logistic model was used (Eq. 3):

$$NTCP = \frac{\exp\left(4\gamma_{50}\left(\frac{Vx}{Vx_{50}} - 1\right)\right)}{1 + \exp\left(4\gamma_{50}\left(\frac{Vx}{Vx_{50}} - 1\right)\right)} \quad 3$$

where Vx is the volume of tissue exceeding x Gy, which is x=12 Gy in Figures 1–5 and x=14 Gy in Figure 6, Vx_{50} is the volume corresponding to 50% risk of necrosis, and γ_{50} is the slope parameter. The best-fitting values were found using maximum likelihood method, and the 95% confidence intervals were calculated using the profile-likelihood method [98].

It was observed that the risk level reported by Korytko et al. [43], in which 44% of lesions developed symptomatic necrosis, was substantially higher than what was reported in the other datasets. Potential causes of the vastly differing reported rates of necrosis are unknown. Therefore, the Korytko et al. dataset was kept separate from the HyTEC model that included the other 4 studies, as seen in Figure 5.

The studies by Inoue et al. [52,53] and Peng et al. [22] included only patients with brain metastases, and comprise the data that are modelled and shown in Figure 6. These 3 studies analyzed two separate endpoints: A) any edema or necrosis, which we have designated as grade 1–3; and B) necrosis requiring surgical resection, allowing pathological confirmation of necrosis, which we have designated as grade 3. The studies from Inoue et al.[52,53] used V14, which was chosen as the dosimetric measure for Figure 6. The Peng et al. study analyzed Vx by patient, while the studies by Inoue et al. analyzed Vx by lesion. Most patients in these studies had a single treated lesion, though specific data on number of lesions per data point in the Peng study is not available. From individual patient/lesion data from these 3 studies, we show the volume response NTCP models (Figure 6) and dose-volume risk data (Table 3) for brain necrosis in patients treated with SRS/fSRS for brain metastases.

It is notable that fSRS was used in some (Peng et al.) or all (Inoue et al.) of the patients in the 3 studies included in the NTCP model for brain metastases. For 1-, 3- and 5-fraction SRS/fSRS, there were 96, 182 and 105 data points, respectively, with a median calculated V14 of 3.9 cc, 11.7 cc and 17.5 cc respectively. For V14 of 0–5 cc, 5–10 cc, 10–20 cc and >20 cc there were 71, 71, 216 and 25 data points, respectively, with single-fraction SRS accounting for 77%, 37%, 6% and 8% of data points, respectively. Thus, the risks for calculated V14>10 cc reflect mostly fSRS data.

Notably, for the modelling shown in Figures 1–4 (section 4), the logarithm of volume V12 was used in the logistic model (Eq. 1) forcing a 0% risk at 0 Gy, whereas no logarithm of volume was used for the modelling shown in Figures 5–6. The different approaches to modelling, as well as using binned data extracted from published studies (Figures 1–

4) versus more granular individual patient data (Figures 5–6) account for the different appearance between these curves. Supplemental Figure S4 shows how the models in Figures 3A–B would be different if logarithm of volumes were not used (i.e., similar to what was done in Figures 5–6).

In a recent HyTEC review for optic nerve and chiasm [99], limitations of the NTCP modelling were discussed in detail. These limitations include statistical uncertainties with data compilation, uncertainties in the α/β value and applicability of the LQ model, and the absence of data in the low-dose and high-dose extremes. Additionally, the inclusion of retrospective studies, with different planning and delivery methods and follow-up protocols is another limitation; with retrospective studies, necrosis could be under-reported.

7. SPECIAL SITUATIONS

Brainstem targets:

It is well-recognized that the brainstem is more susceptible to symptomatic radiation toxicity; some studies in this analysis [24,25,32,34,36,48], the AAPM Task Group101 report [100] and QUANTEC paper [101] suggest relatively stringent SRS/fSRS constraints for brainstem. While several of the studies in our analyses included brainstem targets, they generally represented only a small percent of patients (e.g.,1% [29,35,40,72] to 2–5% [36,39,45,47,48,61] in most studies). Exceptions are studies from the University of Pittsburgh [24,34] and Gunma University [52,53] (~17–25% with brainstem lesions; see Supplemental Table 1). The most recent AVM study from the University of Pittsburgh [32] included 55 (7%) of 755 brainstem AVMs. Other studies of fSRS described including some brain lesions abutting the brainstem [27,50,54,66]. Because we explicitly omitted studies that focused of brainstem toxicity, we have not reported specific dose-volume metrics predictive of brainstem toxicity.

Notably, in a recent multi-institutional pooled analysis [102] of 547 patients with 596 brainstem metastases treated with Gamma-Knife SRS, 7.4% of lesions developed grade 3+ toxicity. Factors associated with significantly increased risks of grade 3+ toxicity included tumor volume >1 ml (odds ratio (OR) >10, $p<0.001$), doses >16 Gy to target margin (OR >3, $p=0.05$) and prior WBRT (OR=4.7, $p=0.002$). No grade 3+ toxicity occurred with margin doses <12 Gy or with tumors <0.1 ml. Primary cancer type ($p>0.2$), brainstem location ($p=0.30$) and tissue V12 ($p=0.06$) were not significant factors.

Resected brain metastases:

In a 2020 study of 442 patients treated with SRS for 501 resection cavities, the 1-year rates of ARE and symptomatic ARE were 8.9% and 5.9%, respectively [103]. In a pooled analysis of 36 studies of post-resection cavity SRS/fSRS, the risk of radionecrosis was 6.9% [104]. Among the 51 reports summarized here, in 10 studies some [30,50] or all [28,49,51,56,63,67,69,70] of the patients underwent SRS (2 studies) or fSRS (10 studies) to the surgical cavity of a resected brain metastasis. For resected brain metastases, the X Gy isodose line volume (i.e., ‘tissue Vx’) may not be as clinically meaningful as brain Vx, given that the target volume likely includes fluid (i.e., non-tissue) within the cavity.

In a 2018 analysis (outside of this report's search) of 90 resection cavities in 80 patients treated with SRS, there were 5 necrosis events; greater necrosis risks were associated with greater brain/parenchymal V12 (p=0.05) and smaller total (i.e. tissue) V12 (p=0.03) [105]. The authors postulated that larger cavities (and therefore greater V12) may have been more likely to border the calvarium or ventricles, accounting for the counter-intuitive finding of lower necrosis risks with greater tissue V12. While patients with intact or subtotally resected brain metastases may develop symptomatic tumor or brain necrosis after SRS/fSRS, in those with completely resected brain metastases, necrosis would only develop within 'normal brain' though this brain may have had tumor- or surgery-related functional impairment prior to SRS/fSRS. In a 2019 study of patients treated with post-op, frameless, LINAC-based 5-fraction fSRS, 10 of 52 (19%) developed radionecrosis, with risks correlated with "hot-spot" doses >105% outside the cavity, and *not* with maximum doses within the CTV; brain V25, V30 and V35 were *not* associated with radionecrosis risks [106]. In a 2020 report, intact metastases were associated with a significant >3-fold higher relative-risk of symptomatic ARE vs. resection cavities (after accounting for brain V30 and other factors) [90].

None of the 10 studies reviewed in this report, that included patients with resected brain metastases, analyzed tissue/total Vx, while 3 studies specifically reported brain Vx [49,51,70]. The study by Broemme et al. [51] reported one event in 44 treatments, and the 'normal brain' V10–12 (in 1 fraction) associated with that event (Supplemental Table 4). The study by Dore et al. [70] reported a range and median of brain (minus PTV) V12 and V21 values (in 3 fractions) among those who did vs. did not develop radiographic evidence of necrosis; V10, V12 and V21 were significantly greater in the group that developed necrosis (Supplemental Table 3); binned groups of V10, V12 and V21, with associated necrosis risks, were not described.

Staged-SRS for AVM:

For bulky AVMs, for which single-fraction SRS (at doses needed for an appreciable likelihood of obliteration) would be associated with unacceptable risks of necrosis, staged-SRS is alternative. One approach is fSRS- termed dose-staged SRS, as the entire target is treated with multiple fractions; another approach is volume-staged SRS, in which segmented portions of the target are treated sequentially, generally months apart. A recent review summarizes the risks of radiation-induced changes as well as death (in part due to hemorrhage risks) [107]. Deep AVM location (i.e., basal ganglia, thalamus, and brainstem) appears to be associated with a 5-fold increased risk of radiation-induced changes vs. other locations [108]. We opted against including staged-SRS in our analyses as nearly all studies published to date have included <50 patients, and have not focused on dose-volume effects on necrosis risks.

Re-irradiation:

While prior WBRT may not appreciably increase the risks of brain toxicity after SRS/fSRS (see section 5), prior SRS/fSRS appears to increase toxicity risks compared to patients with no prior radiotherapy [29,73,109]. For example, in a study from UCSF, prior SRS increased toxicity risks ~5-fold [29]; in those with vs. without prior SRS, crude rates of ARE were 14% vs. 3%, respectively, and 1-year cumulative incidences of ARE were 20%

vs. 4%, respectively. A retrospective analysis, from Wake Forest of 32 patients with 46 lesions receiving 2 courses of SRS, suggested that tissue composite V40 was associated (p=0.003) with the development of radionecrosis. The composite V40 values (sum from 2 single-fraction SRS plans) of 0.28, 0.76 and 1.60 cc were associated with 10%, 20%, and 50% probabilities of radionecrosis, respectively [110]. Other reports of repeated courses of SRS suggest that retreatment is tolerable for AVMs and brain metastases [111–115]. We did not analyze or model the effect of repeat SRS due to limited data. As dosimetric predictors of toxicity after repeat SRS are limited, caution is warranted when considering re-irradiation.

Concurrent systemic therapy:

Data on concurrent systemic therapy and cranial SRS, while limited, suggest that concurrent cranial SRS and cytotoxic chemotherapy may not increase risk of neurotoxicity or radionecrosis [116,117], and may decrease risks [118]. In a retrospective study of 1,650 patients with brain metastases treated at the Cleveland Clinic, the 1-year cumulative incidence of necrosis was 6.6% in the lesions treated with SRS concurrently with a variety of systemic therapies, vs. 5.3% in those treated *without* concurrent systemic therapies (p = 0.14) [116]. Among those who also had received WBRT, radionecrosis rates were significantly elevated with concurrent SRS and systemic therapy, while there was no significant effect of systemic therapy on necrosis risks among those treated with SRS alone. Notably, on subset analyses, significantly increased risks of post-SRS necrosis were observed with concurrent VEGFR and EGRF tyrosine kinase inhibitors (necrosis rates 14–16%) as well as HER2 antibodies. Thus, it is prudent to consider withholding these specific agents when delivering SRS. Despite ALK rearrangement being associated with radionecrosis risks in the aforementioned study from Cleveland Clinic, the use of ALK inhibitors was not [93]. In the absence of more data, systemic therapy immediately before and after SRS/fSRS should only be considered with caution.

Concurrent immunotherapy:

Immune checkpoint inhibitors (ICI) have a long duration of potential efficacy and may act synergistically with SRS, potentially exacerbating toxicity risks [119]. Concurrent SRS and ICI was not associated with increased risks of adverse events in studies from Johns Hopkins [120], Yale [118] or University of Virginia [121], though a study from Harvard [122] suggested that ICI may increase risks of post-SRS radionecrosis. A 2019 meta-analysis reported a 0–21% risk of radionecrosis (among 5 studies) in patients with brain metastases treated with SRS and ICI, with risks possibly related to the specific agents used; data were too limited to elucidate a temporal relationship between SRS and ICI [123]. Investigators from Wake Forest showed, among 289 patients with 2004 brain metastases, that while receipt of immune checkpoint inhibitors increased risks of adverse radiation effects (HR=2.58, p<0.01), the timing of receipt of immune checkpoint inhibitors (within 30 days or not) was not a significant factor [124]. Many randomized controlled trials evaluating the safety and efficacy of ICI and SRS for brain metastases are accruing [125].

Pediatric patients:

Our analyses did not specifically address brain toxicity after SRS/fSRS in the pediatric population due to insufficient data.

8. RECOMMENDED DOSE/VOLUME OBJECTIVES

For brain metastases treated with SRS, our analyses suggest that the risks of grade 3 necrosis are approximately 0.4%, 0.8% and 3.4% for the total irradiated volumes (including target volume) receiving a single-fraction equivalent dose of 14 Gy (V14) of 5 cc, 10 cc and 20 cc, respectively. These data can be used in conjunction with much of the published data that focused on V10–12 (with V12 shown in Figures 1–4 and Supplemental Figures S1–3), as described below.

It is notable that fSRS was used in 3 of the studies included in our NTCP model, and accounted for >90% of the V14>10 cc data. Thus, our modelled ~3.4% risk of grade 3 toxicity for a V14 of 20 cc would be most applicable to multi-fraction regimens, approximately corresponding to a V23 in 3 fractions and V29 in 5 fractions (using the LQ model with alpha-beta ratio of 2 Gy). A recent meta-analysis of 24 studies demonstrated that fSRS for large (>4 cc) brain metastases reduced the risk of radionecrosis (at prescribed doses that did not compromise tumor control probability) relative to commonly used single-fraction SRS doses [87]. We similarly note significantly reduced NTCP with fSRS vs. SRS. These findings suggest that the LQ model may overestimate the single-fraction dose equivalent for NTCP.

Thus, the QUANTEC recommendation to limit single-fraction V12Gy to ≤5–10 cc [20] remains prudent, particularly since the QUANTEC model was based solely on single-fraction SRS data (without the uncertainties with dose conversions), and in light of the high risks reported in the Korytko et al. series [43]. From our compiled data from published studies, the risk of symptomatic necrosis with a V12 of 10 cc is on the order of 15% after SRS for brain metastases (Figure 4 and Supplemental Figure S3), and ~10% after SRS for AVM (Figure 2); though risks appear to be location-dependent [25] which we did not account for. Notably, after fSRS for brain metastases, a single-fraction equivalent V12 of 10 cc is associated with a ~5–10% of symptomatic necrosis (Figure 4 and Supplemental Figure S3).

The recent UK Consensus on Normal Tissue Dose Constraints project [126] and UK Consortium SABR guidelines (version 6.1) [127] recommended a dose of <12 Gy in 1 fraction to 10 cc of brain minus GTV (D10<12 Gy; which would result in a brain V12<10 cc). The AAPM Task Group 101 report did not include specific SRS/fSRS constraints for brain parenchyma [100]. The QUANTEC authors [20] noted substantial variation between studies and emphasized that “more stringent constraints are needed for eloquent brain regions such as brainstem and corpus callosum.” Nevertheless, decisions for individual patients should weigh their goals of care as well as NTCP and TCP estimates. Prescribing more ‘moderate’ fSRS/SRS doses for brain metastases (relative to commonly prescribed dose schedules), in an effort to reduce radionecrosis risks may be considered for select patients [128], more study is needed to determine the optimal dose-fractionation schemes

with respect to NTCP and TCP. There is a separate HYTEC TCP effort for brain metastases that might help guide these often-challenging decisions regarding balancing NTCP and TCP.

9. FUTURE STUDIES

Future retrospective and prospective studies should utilize consistent reporting standards (outlined in section 10). More consistent means of establishing the diagnosis of radionecrosis versus tumor progression are needed, as different institutions utilize different imaging modalities. Also, the endpoints of ARE (which can be temporary) vs. necrosis (which reflects tissue injury) are challenging to characterize at the onset, since it is often unknown if the symptoms and/or imaging changes will be reversible or not [29]. Large patient numbers, and data pooling, are needed to sort out which variables, in addition to dose and volume, affect risk of symptomatic necrosis. Of particular interest would be a better description of susceptibility to necrosis/edema in different regions of the brain for brain metastases patients, similar to the efforts by Flickinger and colleagues for AVMs [25,129]. Whether necrosis risks are technology/platform dependent should be studied further [130–132], though differences in risks are potentially subject to institutional variations in planning practices (even with the same technology) as well as new and continually evolving technologies. The American Society for Radiation Oncology (ASTRO) and the American Association of Neurological Surgeons (AANS) SRS registry may facilitate pooled analyses, utilizing clinical and dosimetric parameters. Actuarial analyses are needed to better understand the time course of risks as well as the long-term actuarial toxicity risks. Patients with brain metastases are living longer than they were in prior decades owing to improved imaging (resulting in diagnosis of smaller volume brain metastases earlier in the course of disease) and improved therapy. Future studies should seek to better identify which patients benefit the most from fSRS vs. SRS with respect to NTCP and TCP, particularly for targets that are smaller and not abutting dose-limiting tissue (i.e. brainstem, optic apparatus), for which scant comparative data exist.

It is important to continue investigating factors that may cause some studies to have higher incidence of necrosis than others, such as grading, histology, and other potential reasons.

10. REPORTING STANDARDS

Necrosis, edema and brain toxicity should be scored using standardized toxicity criteria. The CTCAE version 4 scores the extent of toxicity. The RANO-BM report describes the need to differentiate progression from post-radiation change, but consensus criteria for defining necrosis are lacking. Standardized reporting for SRS is needed, and reportedly forthcoming [133]. Ideally the details should be reported per treatment course and per lesion for all patients whether they had toxicity or not, so the denominator of all cases would be known. With respect to toxicity reporting, we propose recording and reporting the following information for patients with and without toxicity (with each bullet point being an item potentially captured in a registry or database):

- Patient age
- Patient sex

- Patient performance status
- Primary tumor type/histology
- Date diagnosed with primary cancer
- Date diagnosed with brain metastases
- Symptoms from brain metastases (Y/N)
- Steroids needed for brain metastases (Y/N)
- Status of extracranial disease (controlled, uncontrolled, new diagnosis)
- Details of prior brain radiotherapy
  - WBRT – Y/N
    - Dates of treatment
    - Fields/technique
    - Dose, fractionation
  - Prior SRS – Y/N
    - target(s)
      - Dates of treatment
      - Prescribed dose
      - Dose-fractionation
      - Controlled (Y/N)
- Details of prior cranial surgery/ies and procedures
  - Prior resection (Y/N)
    - Lesion(s) resected
      - Date of surgery
      - Surgical technique
- Details of SRS tumor(s)/target(s)
  - Intact vs. resected metastasis
  - Tumor/target volumes
  - Location(s) of treated targets/lesions
- Treatment planning parameters
  - Planning software (with version)
  - Planning technique
  - Dose calculation algorithm used
  - Dose calculation grid size (more relevant for small targets)

- Methods of treatment set-up and positional verification
- Target and brain dose metrics and/or DVH
  - Maximum target dose (for each target if applicable)
  - Prescription target dose (for each target if applicable)
  - Dose coverage of each target
    - Percent isodose line covering percent target volume
  - Brain/tissue dose-volume exposure per lesion or per plan, or at least per stratified groups of patients (e.g. quartiles)
    - Tissue Vx across broad range of doses
    - Brain Vx across broad range of doses (with specification of definition of brain (i.e., brain minus GTV or PTV)
    - For multi-lesion treatment: description of lesion Vx and patient (i.e., composite) Vx. For patients with lesions in close proximity, it may not be feasible to specify a lesion Vx, particularly if 2 or more lesions are treated as one target, but also if each lesion is planned as separate targets (due to overlapping isodose lines).
    - Physical dose including fractionation for each reported Vx is preferable (e.g. V12Gy/1fx or V20Gy/3fx, etc.); even when elaborate radiobiological conversions are feasible the basic physical dose and fractionation should also be reported to enable future data pooling initiatives
- Dates of clinical and radiographic follow-up
- Imaging studies used to determine control and toxicity
- Control of tumor or obliteration of AVM (Y/N)
- Toxicity (including adverse imaging changes in the absence of symptoms)
  - Yes/No for each type of event
  - If Yes, specify
    - Date of onset
    - If >1 lesion/target, specify (if possible) which target is the cause of the event
    - Grade (CTC-AE version 4 preferred)
      - no intervention
      - medical intervention
      - surgical intervention

- date
- Criteria used to define toxicity
  - computerized tomography (CT) scan (Y/N)
  - MR imaging (Y/N)
  - Other imaging (Y/N)
  - Symptoms/exam (Y/N)
    - Type of symptoms
- Intervention (Y/N)

  If yes- specify type
- If available: Patient-reported outcomes score
- If available: Data from validated questionnaires such as FACT-BR

As recommended by other HYTEC reports [134], these data should be provided in electronic supplements to facilitate data pooling and NTCP modelling.

Supplementary Material

Refer to Web version on PubMed Central for supplementary material.

REFERENCES

[1]. Fabiano AJ, Prasad D Qiu J. Adverse radiation effect in the brain during cancer radiotherapy. J Radiat Cancer Res 2017;8:135–140.

[2]. Schultheiss TE, Kun LE, Ang KK, et al. Radiation response of the central nervous system. Int J Radiat Oncol Biol Phys 1995;31:1093–1112. [PubMed: 7677836]

[3]. Chao ST, Ahluwalia MS, Barnett GH, et al. Challenges with the diagnosis and treatment of cerebral radiation necrosis. Int J Radiat Oncol Biol Phys 2013;87:449–457. [PubMed: 23790775]

[4]. Mehta S, Shah A Jung H. Diagnosis and treatment options for sequelae following radiation treatment of brain tumors. Clinical neurology and neurosurgery 2017;163:1–8. [PubMed: 29028584]

[5]. Vellayappan B, Tan CL, Yong C, et al. Diagnosis and management of radiation necrosis in patients with brain metastases. Front Oncol 2018;8:395. [PubMed: 30324090]

[6]. Tye K, Engelhard HH, Slavin KV, et al. An analysis of radiation necrosis of the central nervous system treated with bevacizumab. J Neurooncol 2014;117:321–327. [PubMed: 24504500]

[7]. Delishaj D, Ursino S, Pasqualetti F, et al. Bevacizumab for the treatment of radiation-induced cerebral necrosis: A systematic review of the literature. J Clin Med Res 2017;9:273–280. [PubMed: 28270886]

[8]. Levin VA, Bidaut L, Hou P, et al. Randomized double-blind placebo-controlled trial of bevacizumab therapy for radiation necrosis of the central nervous system. Int J Radiat Oncol Biol Phys 2011;79:1487–1495. [PubMed: 20399573]

[9]. Zach L, Guez D, Last D, et al. Delayed contrast extravasation mri: A new paradigm in neuro-oncology. Neuro Oncol 2015;17:457–465. [PubMed: 25452395]

[10]. Zhang Z, Yang J, Ho A, et al. A predictive model for distinguishing radiation necrosis from tumour progression after gamma knife radiosurgery based on radiomic features from mr images. Eur Radiol 2018;28:2255–2263. [PubMed: 29178031]

[11]. Zhou M, Scott J, Chaudhury B, et al. Radiomics in brain tumor: Image assessment, quantitative feature descriptors, and machine-learning approaches. AJNR Am J Neuroradiol 2018;39:208–216. [PubMed: 28982791]

[12]. Peng L, Parekh V, Huang P, et al. Distinguishing true progression from radionecrosis after stereotactic radiation therapy for brain metastases with machine learning and radiomics. Int J Radiat Oncol Biol Phys 2018;102:1236–1243. [PubMed: 30353872]

[13]. Stockham AL, Ahluwalia M, Reddy CA, et al. Results of a questionnaire regarding practice patterns for the diagnosis and treatment of intracranial radiation necrosis after srs. J Neurooncol 2013;115:469–475. [PubMed: 24045970]

[14]. Lin NU, Lee EQ, Aoyama H, et al. Response assessment criteria for brain metastases: Proposal from the rano group. Lancet Oncol 2015;16:e270–278. [PubMed: 26065612]

[15]. Okada H, Weller M, Huang R, et al. Immunotherapy response assessment in neuro-oncology: A report of the rano working group. Lancet Oncol 2015;16:e534–e542. [PubMed: 26545842]

[16]. Cox JD, Stetz J Pajak TF. Toxicity criteria of the radiation therapy oncology group (rtog) and the european organization for research and treatment of cancer (eortc). Int J Radiat Oncol Biol Phys 1995;31:1341–1346. [PubMed: 7713792]

[17]. Trotti A, Colevas AD, Setser A, et al. Ctcae v3.0: Development of a comprehensive grading system for the adverse effects of cancer treatment. Semin Radiat Oncol 2003;13:176–181. [PubMed: 12903007]

[18]. Moher D, Liberati A, Tetzlaff J, et al. Preferred reporting items for systematic reviews and meta-analyses: The prisma statement. PLoS Med 2009;6:e1000097. [PubMed: 19621072]

[19]. Lent soma scales for all anatomic sites. Int J Radiat Oncol Biol Phys 1995;31:1049–1091. [PubMed: 7713776]

[20]. Lawrence YR, Li XA, el Naqa I, et al. Radiation dose-volume effects in the brain. Int J Radiat Oncol Biol Phys 2010;76:S20–27. [PubMed: 20171513]

[21]. Reynolds TA, Jensen AR, Bellairs EE, et al. Dose gradient index for stereotactic radiosurgery/radiation therapy. Int J Radiat Oncol Biol Phys 2020;106:604–611. [PubMed: 32014151]

[22]. Peng L, Grimm J, Gui C, et al. Updated risk models demonstrate low risk of symptomatic radionecrosis following stereotactic radiosurgery for brain metastases in the modern era. Surgical Neurology International 2018;10:32.

[23]. Milano MT, Sharma M, Soltys SG, et al. Radiation-induced edema after single-fraction or multifraction stereotactic radiosurgery for meningioma: A critical review. Int J Radiat Oncol Biol Phys 2018;101:344–357. [PubMed: 29726362]

[24]. Flickinger JC, Kondziolka D, Maitz AH, et al. Analysis of neurological sequelae from radiosurgery of arteriovenous malformations: How location affects outcome. Int J Radiat Oncol Biol Phys 1998;40:273–278. [PubMed: 9457809]

[25]. Flickinger JC, Kondziolka D, Lunsford LD, et al. Development of a model to predict permanent symptomatic postradiosurgery injury for arteriovenous malformation patients. Arteriovenous malformation radiosurgery study group. Int J Radiat Oncol Biol Phys 2000;46:1143–1148. [PubMed: 10725624]

[26]. Fahrig A, Ganslandt O, Lambrecht U, et al. Hypofractionated stereotactic radiotherapy for brain metastases--results from three different dose concepts. Strahlenther Onkol 2007;183:625–630. [PubMed: 17960338]

[27]. Inoue HK, Sato H, Suzuki Y, et al. Optimal hypofractionated conformal radiotherapy for large brain metastases in patients with high risk factors: A single-institutional prospective study. Radiat Oncol 2014;9:231. [PubMed: 25322826]

[28]. Eaton BR, La Riviere MJ, Kim S, et al. Hypofractionated radiosurgery has a better safety profile than single fraction radiosurgery for large resected brain metastases. J Neurooncol 2015;123:103–111. [PubMed: 25862006]

[29]. Sneed PK, Mendez J, Vemer-van den Hoek JG, et al. Adverse radiation effect after stereotactic radiosurgery for brain metastases: Incidence, time course, and risk factors. J Neurosurg 2015:1–14.

[30]. Patel KR, Burri SH, Asher AL, et al. Comparing preoperative with postoperative stereotactic radiosurgery for resectable brain metastases: A multi-institutional analysis. Neurosurgery 2016;79:279–285. [PubMed: 26528673]

[31]. Voges J, Treuer H, Lehrke R, et al. Risk analysis of linac radiosurgery in patients with arteriovenous malformation (avm). Acta Neurochir Suppl 1997;68:118–123. [PubMed: 9233426]

[32]. Kano H, Flickinger JC, Tonetti D, et al. Estimating the risks of adverse radiation effects after gamma knife radiosurgery for arteriovenous malformations. Stroke 2017;48:84–90. [PubMed: 27899758]

[33]. Lax I Karlsson B Prediction of complications in gamma knife radiosurgery of arteriovenous malformation. Acta Oncol 1996;35:49–55. [PubMed: 8619940]

[34]. Flickinger JC, Kondziolka D, Pollock BE, et al. Complications from arteriovenous malformation radiosurgery: Multivariate analysis and risk modeling. Int J Radiat Oncol Biol Phys 1997;38:485–490. [PubMed: 9231670]

[35]. Miyawaki L, Dowd C, Wara W, et al. Five year results of linac radiosurgery for arteriovenous malformations: Outcome for large avms. Int J Radiat Oncol Biol Phys 1999;44:1089–1106. [PubMed: 10421543]

[36]. Barker FG 2nd, Butler WE, Lyons S, et al. Dose-volume prediction of radiation-related complications after proton beam radiosurgery for cerebral arteriovenous malformations. J Neurosurg 2003;99:254–263. [PubMed: 12924697]

[37]. Friedman WA, Bova FJ, Bollampally S, et al. Analysis of factors predictive of success or complications in arteriovenous malformation radiosurgery. Neurosurgery 2003;52:296–307; discussion 307–298. [PubMed: 12535357]

[38]. Levegrun S, Hof H, Essig M, et al. Radiation-induced changes of brain tissue after radiosurgery in patients with arteriovenous malformations: Correlation with dose distribution parameters. Int J Radiat Oncol Biol Phys 2004;59:796–808. [PubMed: 15183483]

[39]. Cetin IA, Ates R, Dhaens J, et al. Retrospective analysis of linac-based radiosurgery for arteriovenous malformations and testing of the flickinger formula in predicting radiation injury. Strahlenther Onkol 2012;188:1133–1138. [PubMed: 23128895]

[40]. Herbert C, Moiseenko V, McKenzie M, et al. Factors predictive of symptomatic radiation injury after linear accelerator-based stereotactic radiosurgery for intracerebral arteriovenous malformations. Int J Radiat Oncol Biol Phys 2012;83:872–877. [PubMed: 22208972]

[41]. Varlotto JM, Flickinger JC, Niranjan A, et al. Analysis of tumor control and toxicity in patients who have survived at least one year after radiosurgery for brain metastases. Int J Radiat Oncol Biol Phys 2003;57:452–464. [PubMed: 12957257]

[42]. Valery CA, Cornu P, Noel G, et al. Predictive factors of radiation necrosis after radiosurgery for cerebral metastases. Stereotact Funct Neurosurg 2003;81:115–119. [PubMed: 14742974]

[43]. Korytko T, Radivoyevitch T, Colussi V, et al. 12 gy gamma knife radiosurgical volume is a predictor for radiation necrosis in non-avm intracranial tumors. Int J Radiat Oncol Biol Phys 2006;64:419–424. [PubMed: 16226848]

[44]. Ernst-Stecken A, Ganslandt O, Lambrecht U, et al. Phase ii trial of hypofractionated stereotactic radiotherapy for brain metastases: Results and toxicity. Radiother Oncol 2006;81:18–24. [PubMed: 16978720]

[45]. Williams BJ, Suki D, Fox BD, et al. Stereotactic radiosurgery for metastatic brain tumors: A comprehensive review of complications. J Neurosurg 2009;111:439–448. [PubMed: 19301968]

[46]. Blonigen BJ, Steinmetz RD, Levin L, et al. Irradiated volume as a predictor of brain radionecrosis after linear accelerator stereotactic radiosurgery. Int J Radiat Oncol Biol Phys 2010;77:996–1001. [PubMed: 19783374]

[47]. Minniti G, Clarke E, Lanzetta G, et al. Stereotactic radiosurgery for brain metastases: Analysis of outcome and risk of brain radionecrosis. Radiat Oncol 2011;6:48. [PubMed: 21575163]

[48]. Ohtakara K, Hayashi S, Nakayama N, et al. Significance of target location relative to the depth from the brain surface and high-dose irradiated volume in the development of brain radionecrosis after micromultileaf collimator-based stereotactic radiosurgery for brain metastases. J Neurooncol 2012;108:201–209. [PubMed: 22392126]

[49]. Minniti G, Esposito V, Clarke E, et al. Multidose stereotactic radiosurgery (9 gy × 3) of the postoperative resection cavity for treatment of large brain metastases. Int J Radiat Oncol Biol Phys 2013;86:623–629. [PubMed: 23683828]

[50]. Eaton BR, Gebhardt B, Prabhu R, et al. Hypofractionated radiosurgery for intact or resected brain metastases: Defining the optimal dose and fractionation. Radiat Oncol 2013;8:135. [PubMed: 23759065]

[51]. Broemme J, Abu-Isa J, Kottke R, et al. Adjuvant therapy after resection of brain metastases. Frameless image-guided linac-based radiosurgery and stereotactic hypofractionated radiotherapy. Strahlenther Onkol 2013;189:765–770. [PubMed: 23934329]

[52]. Inoue HK, Seto K, Nozaki A, et al. Three-fraction cyberknife radiotherapy for brain metastases in critical areas: Referring to the risk evaluating radiation necrosis and the surrounding brain volumes circumscribed with a single dose equivalence of 14 gy (v14). J Radiat Res 2013;54:727–735. [PubMed: 23404206]

[53]. Inoue HK, Sato H, Seto K, et al. Five-fraction cyberknife radiotherapy for large brain metastases in critical areas: Impact on the surrounding brain volumes circumscribed with a single dose equivalent of 14 gy (v14) to avoid radiation necrosis. J Radiat Res 2014;55:334–342. [PubMed: 24187332]

[54]. Minniti G, D'Angelillo RM, Scaringi C, et al. Fractionated stereotactic radiosurgery for patients with brain metastases. J Neurooncol 2014;117:295–301. [PubMed: 24488446]

[55]. Schuttrumpf LH, Niyazi M, Nachbichler SB, et al. Prognostic factors for survival and radiation necrosis after stereotactic radiosurgery alone or in combination with whole brain radiation therapy for 1–3 cerebral metastases. Radiat Oncol 2014;9:105. [PubMed: 24885624]

[56]. Ahmed KA, Freilich JM, Abuodeh Y, et al. Fractionated stereotactic radiotherapy to the postoperative cavity for radioresistant and radiosensitive brain metastases. J Neurooncol 2014;118:179–186. [PubMed: 24604750]

[57]. Kirkpatrick JP, Wang Z, Sampson JH, et al. Defining the optimal planning target volume in image-guided stereotactic radiosurgery of brain metastases: Results of a randomized trial. Int J Radiat Oncol Biol Phys 2015;91:100–108. [PubMed: 25442342]

[58]. Cho YH, Lee JM, Lee D, et al. Experiences on two different stereotactic radiosurgery modalities of gamma knife and cyberknife in treating brain metastases. Acta neurochirurgica 2015;157:2003–2009. [PubMed: 26381540]

[59]. Jeong WJ, Park JH, Lee EJ, et al. Efficacy and safety of fractionated stereotactic radiosurgery for large brain metastases. Journal of Korean Neurosurgical Society 2015;58:217–224. [PubMed: 26539264]

[60]. Zhuang H, Zheng Y, Wang J, et al. Analysis of risk and predictors of brain radiation necrosis after radiosurgery. Oncotarget 2016;7:7773–7779. [PubMed: 26675376]

[61]. Nichol A, Ma R, Hsu F, et al. Volumetric radiosurgery for 1 to 10 brain metastases: A multicenter, single-arm, phase 2 study. Int J Radiat Oncol Biol Phys 2016;94:312–321. [PubMed: 26678660]

[62]. Hanna A, Boggs DH, Kwok Y, et al. What predicts early volumetric edema increase following stereotactic radiosurgery for brain metastases? J Neurooncol 2016;127:303–311. [PubMed: 26721241]

[63]. Abuodeh Y, Ahmed KA, Naghavi AO, et al. Postoperative stereotactic radiosurgery using 5-gy × 5 sessions in the management of brain metastases. World Neurosurg 2016;90:58–65. [PubMed: 26921701]

[64]. Ishihara T, Yamada K, Harada A, et al. Hypofractionated stereotactic radiotherapy for brain metastases from lung cancer : Evaluation of indications and predictors of local control. Strahlenther Onkol 2016;192:386–393. [PubMed: 27169391]

[65]. Minniti G, Scaringi C, Paolini S, et al. Single-fraction versus multifraction (3 × 9 gy) stereotactic radiosurgery for large (>2 cm) brain metastases: A comparative analysis of local control and risk of radiation-induced brain necrosis. Int J Radiat Oncol Biol Phys 2016;95:1142–1148. [PubMed: 27209508]

[66]. Navarria P, Pessina F, Cozzi L, et al. Hypo-fractionated stereotactic radiotherapy alone using volumetric modulated arc therapy for patients with single, large brain metastases unsuitable for surgical resection. Radiat Oncol 2016;11:76. [PubMed: 27249940]

[67]. Pessina F, Navarria P, Cozzi L, et al. Outcome evaluation of oligometastatic patients treated with surgical resection followed by hypofractionated stereotactic radiosurgery (hsrs) on the tumor bed, for single, large brain metastases. PloS one 2016;11:e0157869. [PubMed: 27348860]

[68]. Bennion NR, Malouff T, Verma V, et al. A comparison of clinical and radiologic outcomes between frame-based and frameless stereotactic radiosurgery for brain metastases. Practical radiation oncology 2016;6:e283–e290. [PubMed: 27523439]

[69]. Lima L, Sharim J, Levin-Epstein R, et al. Hypofractionated stereotactic radiosurgery and radiotherapy to large resection cavity of metastatic brain tumors. World Neurosurg 2017;97:571–579. [PubMed: 27777153]

[70]. Dore M, Martin S, Delpon G, et al. Stereotactic radiotherapy following surgery for brain metastasis: Predictive factors for local control and radionecrosis. Cancer radiotherapie : journal de la Societe francaise de radiotherapie oncologique 2017;21:4–9. [PubMed: 27955888]

[71]. Voges J, Treuer H, Sturm V, et al. Risk analysis of linear accelerator radiosurgery. Int J Radiat Oncol Biol Phys 1996;36:1055–1063. [PubMed: 8985027]

[72]. Nakamura JL, Verhey LJ, Smith V, et al. Dose conformity of gamma knife radiosurgery and risk factors for complications. Int J Radiat Oncol Biol Phys 2001;51:1313–1319. [PubMed: 11728692]

[73]. Chin LS, Ma L DiBiase S. Radiation necrosis following gamma knife surgery: A case-controlled comparison of treatment parameters and long-term clinical follow up. J Neurosurg 2001;94:899–904. [PubMed: 11409517]

[74]. Ganz JC, Reda WA Abdelkarim K. Adverse radiation effects after gamma knife surgery in relation to dose and volume. Acta neurochirurgica 2009;151:9–19. [PubMed: 19129961]

[75]. Kjellberg RN, Hanamura T, Davis KR, et al. Bragg-peak proton-beam therapy for arteriovenous malformations of the brain. N Engl J Med 1983;309:269–274. [PubMed: 6306463]

[76]. Marks LB Spencer DP. The influence of volume on the tolerance of the brain to radiosurgery. J Neurosurg 1991;75:177–180. [PubMed: 2072155]

[77]. Flickinger JC. An integrated logistic formula for prediction of complications from radiosurgery. Int J Radiat Oncol Biol Phys 1989;17:879–885. [PubMed: 2777680]

[78]. Flickinger JC, Schell MC Larson DA. Estimation of complications for linear accelerator radiosurgery with the integrated logistic formula. Int J Radiat Oncol Biol Phys 1990;19:143–148. [PubMed: 2199419]

[79]. Flickinger JC, Lunsford LD Kondziolka D. Dose-volume considerations in radiosurgery. Stereotact Funct Neurosurg 1991;57:99–105. [PubMed: 1667045]

[80]. Flickinger JC, Lunsford LD, Wu A, et al. Predicted dose-volume isoeffect curves for stereotactic radiosurgery with the 60co gamma unit. Acta Oncol 1991;30:363–367. [PubMed: 2036248]

[81]. Starke RM, Kano H, Ding D, et al. Stereotactic radiosurgery for cerebral arteriovenous malformations: Evaluation of long-term outcomes in a multicenter cohort. J Neurosurg 2017:1–9.

[82]. Shaw E, Scott C, Souhami L, et al. Single dose radiosurgical treatment of recurrent previously irradiated primary brain tumors and brain metastases: Final report of rtog protocol 90–05. Int J Radiat Oncol Biol Phys 2000;47:291–298. [PubMed: 10802351]

[83]. Mohammadi AM, Schroeder JL, Angelov L, et al. Impact of the radiosurgery prescription dose on the local control of small (2 cm or smaller) brain metastases. J Neurosurg 2017;126:735–743. [PubMed: 27231978]

[84]. Amsbaugh M, Pan J, Yusuf MB, et al. Dose-volume response relationship for brain metastases treated with frameless single-fraction linear accelerator-based stereotactic radiosurgery. Cureus 2016;8:e587. [PubMed: 27284495]

[85]. Shehata MK, Young B, Reid B, et al. Stereotatic radiosurgery of 468 brain metastases < or =2 cm: Implications for srs dose and whole brain radiation therapy. Int J Radiat Oncol Biol Phys 2004;59:87–93. [PubMed: 15093903]

[86]. Shuryak I, Carlson DJ, Brown JM, et al. High-dose and fractionation effects in stereotactic radiation therapy: Analysis of tumor control data from 2965 patients. Radiother Oncol 2015;115:327–334. [PubMed: 26058991]

[87]. Lehrer EJ, Peterson JL, Zaorsky NG, et al. Single versus multifraction stereotactic radiosurgery for large brain metastases: An international meta-analysis of 24 trials. Int J Radiat Oncol Biol Phys 2018.

[88]. Kim KH, Kong DS, Cho KR, et al. Outcome evaluation of patients treated with fractionated gamma knife radiosurgery for large (> 3 cm) brain metastases: A dose-escalation study. J Neurosurg 2019:1–10.

[89]. Dohm A, McTyre ER, Okoukoni C, et al. Staged stereotactic radiosurgery for large brain metastases: Local control and clinical outcomes of a one-two punch technique. Neurosurgery 2017;83:114–121.

[90]. Faruqi S, Ruschin M, Soliman H, et al. Adverse radiation effect after hypofractionated stereotactic radiosurgery in 5 daily fractions for surgical cavities and intact brain metastases. Int J Radiat Oncol Biol Phys 2020;106:772–779. [PubMed: 31928848]

[91]. Minniti G, Capone L, Nardiello B, et al. Neurological outcome and memory performance in patients with 10 or more brain metastases treated with frameless linear accelerator (linac)-based stereotactic radiosurgery. J Neurooncol 2020;148:47–55. [PubMed: 32100230]

[92]. Milano MT, Usuki KY, Walter KA, et al. Stereotactic radiosurgery and hypofractionated stereotactic radiotherapy: Normal tissue dose constraints of the central nervous system. Cancer Treat Rev 2011;37:567–578. [PubMed: 21571440]

[93]. Miller JA, Bennett EE, Xiao R, et al. Association between radiation necrosis and tumor biology after stereotactic radiosurgery for brain metastasis. Int J Radiat Oncol Biol Phys 2016;96:1060–1069. [PubMed: 27742540]

[94]. Prabhu RS, Press RH, Patel KR, et al. Single-fraction stereotactic radiosurgery (srs) alone versus surgical resection and srs for large brain metastases: A multi-institutional analysis. Int J Radiat Oncol Biol Phys 2017;99:459–467. [PubMed: 28871997]

[95]. Ma L, Petti PL, Smith V, et al. Functional relationship between the volume of a near-target peripheral isodose line and its dose value for gamma knife radiosurgery, vol. 1, 2007.

[96]. Ma L, Sahgal A, Descovich M, et al. Equivalence in dose fall-off for isocentric and nonisocentric intracranial treatment modalities and its impact on dose fractionation schemes. Int J Radiat Oncol Biol Phys 2010;76:943–948. [PubMed: 20159366]

[97]. Okunieff P, Morgan D, Niemierko A, et al. Radiation dose-response of human tumors. Int J Radiat Oncol Biol Phys 1995;32:1227–1237. [PubMed: 7607946]

[98]. Levegrun S, Jackson A, Zelefsky MJ, et al. Fitting tumor control probability models to biopsy outcome after three-dimensional conformal radiation therapy of prostate cancer: Pitfalls in deducing radiobiologic parameters for tumors from clinical data. Int J Radiat Oncol Biol Phys 2001;51:1064–1080. [PubMed: 11704332]

[99]. Milano MT, Grimm J, Soltys SG, et al. Single- and multi-fraction stereotactic radiosurgery dose tolerances of the optic pathways. Int J Radiat Oncol Biol Phys 2018.

[100]. Benedict SH, Yenice KM, Followill D, et al. Stereotactic body radiation therapy: The report of aapm task group 101. Med Phys 2010;37:4078–4101. [PubMed: 20879569]

[101]. Mayo C, Yorke E Merchant TE. Radiation associated brainstem injury. Int J Radiat Oncol Biol Phys 2010;76:S36–41. [PubMed: 20171516]

[102]. Trifiletti DM, Lee CC, Kano H, et al. Stereotactic radiosurgery for brainstem metastases: An international cooperative study to define response and toxicity. Int J Radiat Oncol Biol Phys 2016;96:280–288. [PubMed: 27478166]

[103]. Shi S, Sandhu N, Jin MC, et al. Stereotactic radiosurgery for resected brain metastases: Single-institutional experience of over 500 cavities. Int J Radiat Oncol Biol Phys 2020;106:764–771. [PubMed: 31785338]

[104]. Akanda ZZ, Hong W, Nahavandi S, et al. Post-operative stereotactic radiosurgery following excision of brain metastases: A systematic review and meta-analysis. Radiother Oncol 2020;142:27–35. [PubMed: 31563407]

[105]. Patel RA, Lock D, Helenowski IB, et al. Postoperative stereotactic radiosurgery for patients with resected brain metastases: A volumetric analysis. J Neurooncol 2018;140:395–401. [PubMed: 30084023]

[106]. Tanenbaum DG, Buchwald ZS, Jhaveri J, et al. Dosimetric factors related to radiation necrosis after 5-fraction radiosurgery for patients with resected brain metastases. Pract Radiat Oncol 2020;10:36–43. [PubMed: 31586666]

[107]. Ilyas A, Chen CJ, Ding D, et al. Radiation-induced changes after stereotactic radiosurgery for brain arteriovenous malformations: A systematic review and meta-analysis. Neurosurgery 2018;83:365–376. [PubMed: 29040700]

[108]. Zengpanpan Y A X Y. C. Letter: Radiation-induced changes after stereotactic radiosurgery for brain arteriovenous malformations: A systematic review and meta-analysis. Neurosurgery 2018;82:E75–76. [PubMed: 29309635]

[109]. Jimenez RB, Alexander BM, Mahadevan A, et al. The impact of different stereotactic radiation therapy regimens for brain metastases on local control and toxicity. Adv Radiat Oncol 2017;2:391–397. [PubMed: 29114607]

[110]. McKay WH, McTyre ER, Okoukoni C, et al. Repeat stereotactic radiosurgery as salvage therapy for locally recurrent brain metastases previously treated with radiosurgery. J Neurosurg 2017;127:148–156. [PubMed: 27494815]

[111]. Awad AJ, Walcott BP, Stapleton CJ, et al. Repeat radiosurgery for cerebral arteriovenous malformations. J Clin Neurosci 2015;22:945–950. [PubMed: 25913746]

[112]. Minniti G, Scaringi C, Paolini S, et al. Repeated stereotactic radiosurgery for patients with progressive brain metastases. J Neurooncol 2016;126:91–97. [PubMed: 26369769]

[113]. Kwon KY, Kong DS, Lee JI, et al. Outcome of repeated radiosurgery for recurrent metastatic brain tumors. Clinical neurology and neurosurgery 2007;109:132–137. [PubMed: 16930821]

[114]. Rana N, Pendyala P, Cleary RK, et al. Long-term outcomes after salvage stereotactic radiosurgery (srs) following in-field failure of initial srs for brain metastases. Front Oncol 2017;7:279. [PubMed: 29218301]

[115]. Koffer P, Chan J, Rava P, et al. Repeat stereotactic radiosurgery for locally recurrent brain metastases. World Neurosurg 2017;104:589–593. [PubMed: 28450235]

[116]. Kim JM, Miller JA, Kotecha R, et al. The risk of radiation necrosis following stereotactic radiosurgery with concurrent systemic therapies. J Neurooncol 2017;133:357–368. [PubMed: 28434110]

[117]. Shen CJ, Kummerlowe MN, Redmond KJ, et al. Stereotactic radiosurgery: Treatment of brain metastasis without interruption of systemic therapy. Int J Radiat Oncol Biol Phys 2016;95:735–742. [PubMed: 27034175]

[118]. Colaco RJ, Martin P, Kluger HM, et al. Does immunotherapy increase the rate of radiation necrosis after radiosurgical treatment of brain metastases? J Neurosurg 2016;125:17–23. [PubMed: 26544782]

[119]. Tran TT, Jilaveanu LB, Omuro A, et al. Complications associated with immunotherapy for brain metastases. Curr Opin Neurol 2019;32:907–916. [PubMed: 31577604]

[120]. Chen L, Douglass J, Kleinberg L, et al. Concurrent immune checkpoint inhibitors and stereotactic radiosurgery for brain metastases in non-small cell lung cancer, melanoma, and renal cell carcinoma. Int J Radiat Oncol Biol Phys 2018;100:916–925. [PubMed: 29485071]

[121]. Shepard MJ, Xu Z, Donahue J, et al. Stereotactic radiosurgery with and without checkpoint inhibition for patients with metastatic non-small cell lung cancer to the brain: A matched cohort study. J Neurosurg 2019:1–8.

[122]. Martin AM, Cagney DN, Catalano PJ, et al. Immunotherapy and symptomatic radiation necrosis in patients with brain metastases treated with stereotactic radiation. JAMA Oncol 2018;4:1123–1124. [PubMed: 29327059]

[123]. Lehrer EJ, Peterson J, Brown PD, et al. Treatment of brain metastases with stereotactic radiosurgery and immune checkpoint inhibitors: An international meta-analysis of individual patient data. Radiother Oncol 2019;130:104–112. [PubMed: 30241791]

[124]. Helis CA, Hughes RT, Glenn CW, et al. Predictors of adverse radiation effect in brain metastasis patients treated with stereotactic radiosurgery and immune checkpoint inhibitor therapy. Int J Radiat Oncol Biol Phys 2020.

[125]. Lehrer EJ, McGee HM, Peterson JL, et al. Stereotactic radiosurgery and immune checkpoint inhibitors in the management of brain metastases. Int J Mol Sci 2018;19.

[126]. Hanna GG, Murray L, Patel R, et al. Uk consensus on normal tissue dose constraints for stereotactic radiotherapy. Clin Oncol (R Coll Radiol) 2018;30:5–14. [PubMed: 29033164]

[127]. Uk consortium: Stereotactic ablative body radiation therapy (sabr): A resource, vol. 2019, ed. version 6.1, 2019.

[128]. Cummings M, Youn P, Bergsma DP, et al. Single-fraction radiosurgery using conservative doses for brain metastases: Durable responses in select primaries with limited toxicity. Neurosurgery 2017;83:437–444.

[129]. Flickinger JC, Kondziolka D, Lunsford LD, et al. A multi-institutional analysis of complication outcomes after arteriovenous malformation radiosurgery. Int J Radiat Oncol Biol Phys 1999;44:67–74. [PubMed: 10219796]

[130]. Sebastian NT, Glenn C, Hughes R, et al. Linear accelerator-based radiosurgery is associated with lower incidence of radionecrosis compared with gamma knife for treatment of multiple brain metastases. Radiother Oncol 2020;147:136–143. [PubMed: 32294607]

[131]. Navarria P C; CG Attuati L, et al. Randomized phase iii trial comparing gamma knife and linac based (edge) approaches for brain metastases radiosurgery: Results from the gadget trial. Int J Radiat Oncol Biol Phys 2018;102:S143.

[132]. Clerici E, Navarria P, Carta GA, et al. Randomized phase iii trial comparing gamma knife (gk) and linac based (edge) radiosurgery for brain metastases from solid tumors: Results from the gadget trial. Neuro-Oncology 2018;20:iii227.

[133]. Chung C, Torrens M, Paddick I, et al. Radiosurgery nomenclature: A confusion of tongues. Int J Radiat Oncol Biol Phys 2015;92:512–513. [PubMed: 26068485]

[134]. Kong FS, Moiseenko V, Zhao J, et al. Organs at risk considerations for thoracic stereotactic body radiation therapy: What is safe for lung parenchyma? Int J Radiat Oncol Biol Phys 2018.

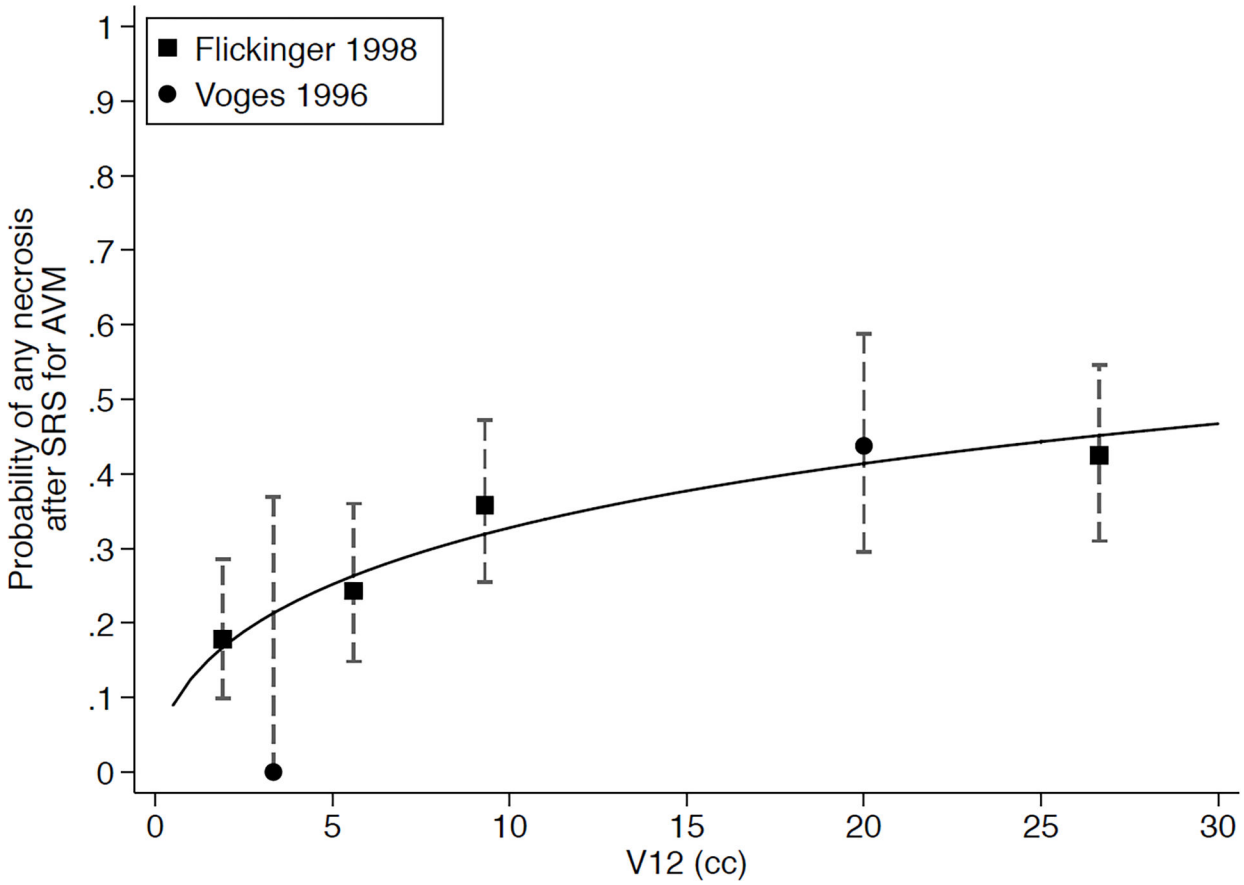

Figure 1.

Risk of any necrosis (symptomatic or asymptomatic) after SRS for AVM vs. tissue volume receiving ≥12 Gy in one fraction (V12). Data were extracted from studies which subgrouped (binned) ranges of V10-V12 and reported the risks of necrosis for patients/lesions within the individual bins. The figure represents a rough approximation of data, as (1) the median value of V12 for a given bin was estimated as the midpoint in the range of values in that bin, except for the bin with the greatest V12; for the largest-value bins, it was assumed that the highest values within that bin represented a relatively small proportion of patients (i.e., the extremely large V12 values were outliers); (2) for data from the Voges et al. study which reported V10, the equivalent to V12 was estimated as described in the text (Eq. 2). The error bars represent 95% binomial confidence intervals and the solid lines represent a fitted logistic model to the data. Studies included Voges, 1996 and Flickinger, 1998; both were single-fraction SRS studies.

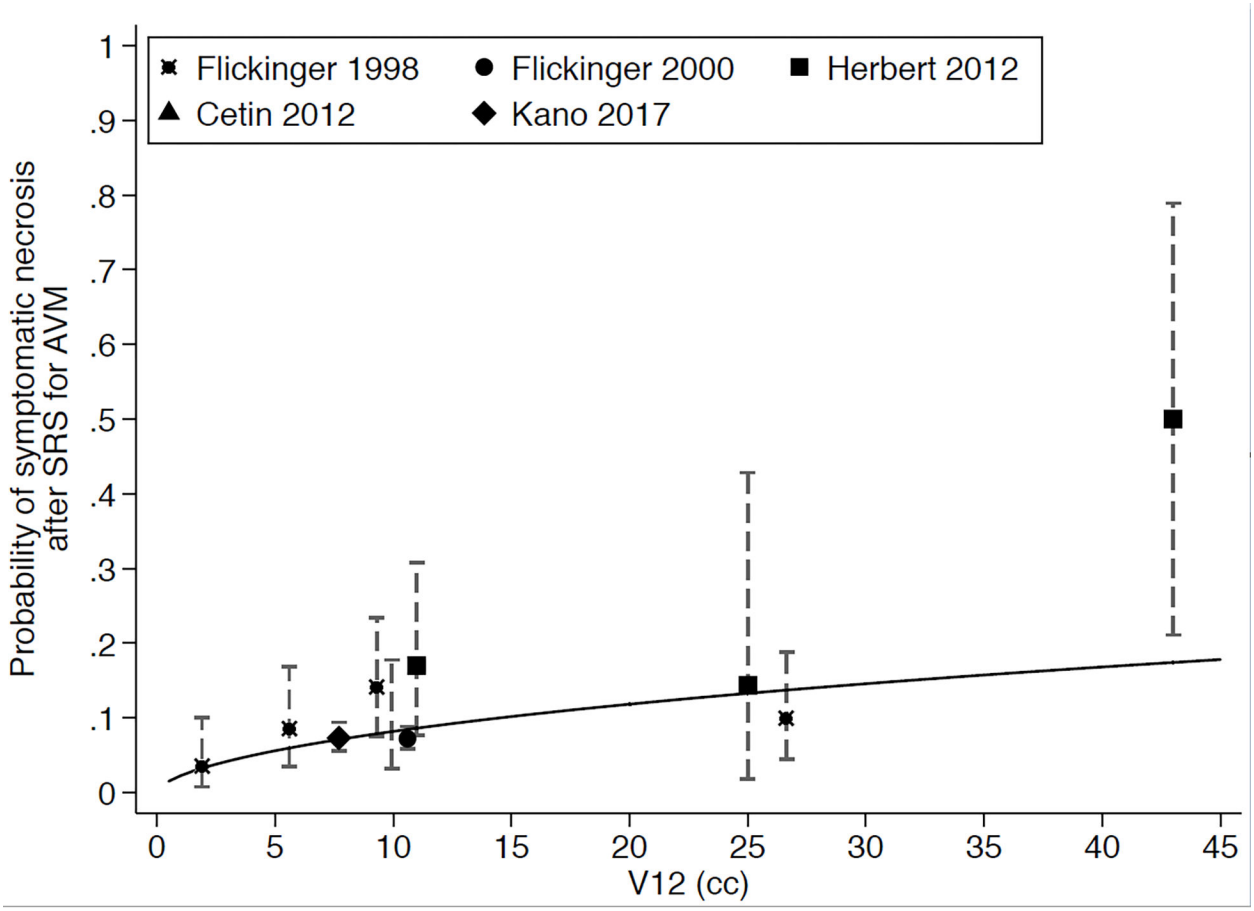

Figure 2.

Risk of symptomatic necrosis after SRS for AVM vs. tissue volume receiving ≥12 Gy in one fraction (V12). Data were extracted from studies that reported necrosis risks and median V12 among all patients or subgrouped (binned) ranges of V12 and reported the risks of necrosis for patients/lesions within the individual bins. The figure represents a rough approximation of data, as the median value of V12 for a given bin was estimated as described in the caption from Figure 1. The error bars represent 95% binomial confidence intervals and the solid lines represent a fitted logistic model to the data. Studies included Flickinger, 1998; Flickinger, 2000; Cetin, 2012; Herbert, 2012; and Kano, 2017; all were single-fraction SRS studies. The data from Herbert et al. was obtained from the authors. Three of the 5 studies included patients from one institution (University of Pittsburgh).

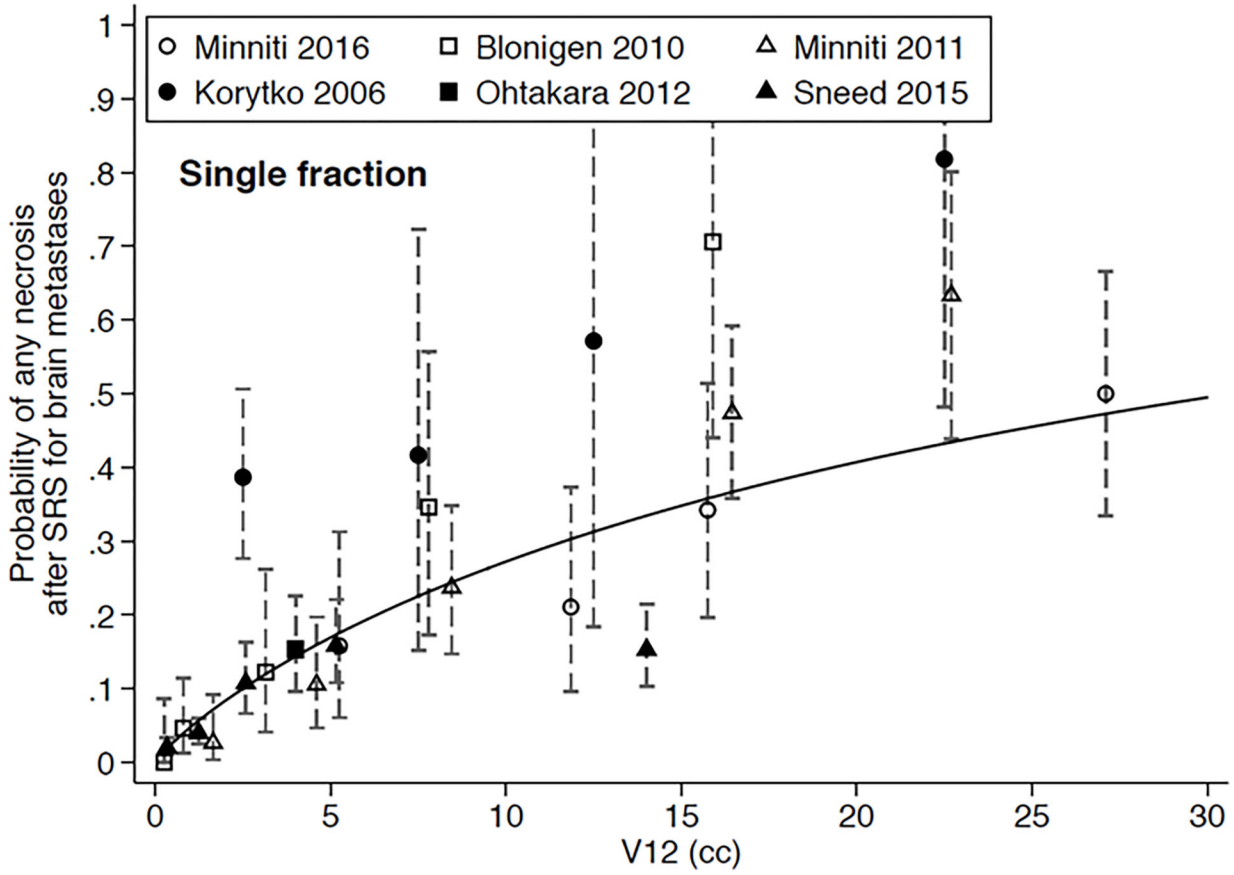

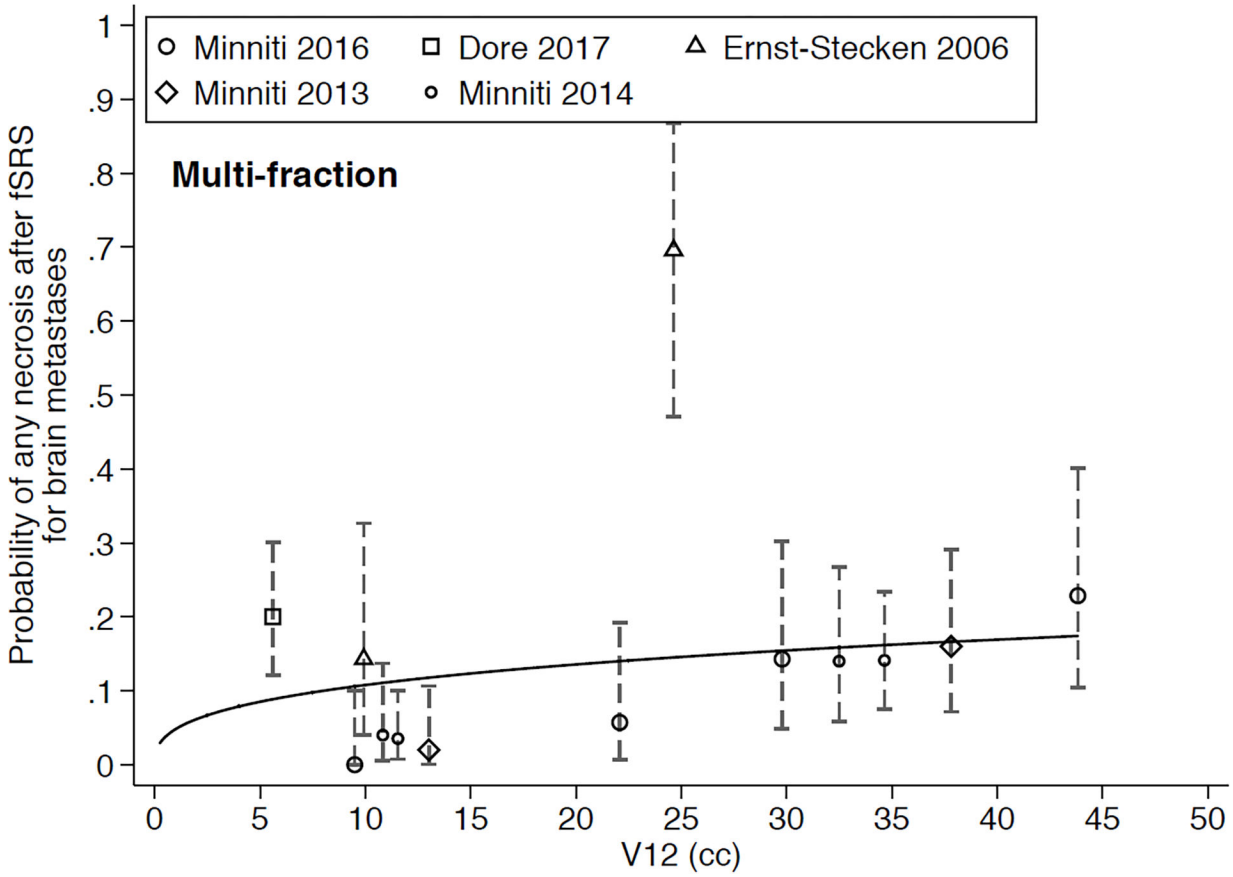

Figure 3.

Risk of any necrosis (symptomatic or asymptomatic) after SRS for brain metastases vs. tissue (target plus non-target) or brain (excluding the target volume and non-brain normal tissue) volume receiving ≥12 Gy equivalent in one fraction (V12). Panel A shows data from single-fraction SRS studies; solid data points represent tissue V12 (target plus non-target) and hollow data points represent brain V12 (excluding the target volume and non-brain normal tissue). Panel B shows data from multi-fraction SRS studies (all reporting brain Vx; i.e. again excluding the target volume and non-brain normal tissue). Data were extracted from studies that reported necrosis risks and median Vx among all patients/lesions or subgrouped (binned) ranges of Vx and reported the risks of necrosis for patients/lesions within the individual bins. One study (Minniti, 2016) in Figure 3A calculated Vx per patient while the others calculated Vx per lesion (see text); all of the studies in Figure 3B calculated Vx per patient. These figures represent a rough approximation of data, as (1) the median value of V12 for a given bin was estimated as described in the caption from Figure 1; (2) for multi-fraction SRS studies, the linear-quadratic model with alpha-beta ratio of 2 was used to convert dose to single-fraction equivalent dose. The error bars represent 95% binomial confidence intervals and the solid lines represent a fitted logistic model to the data. When analyzed separately, there was no significant difference between the tissue V12 and brain V12 logistic models; they are therefore combined together in Panel A, recognizing that tissue V12 would have a larger value than brain V12, and that the figure is meant to be descriptive. Studies included in Figure 3A were Korytko, 2006; Blonigen, 2010; Minniti,

2011; Ohtakara, 2012; Sneed, 2015; Minniti, 2016. Studies included in Figure 3B were Ernst-Stecken, 2006; Minniti, 2013 (with 1 resected brain metastasis per patient); Minniti, 2014; Minniti, 2016; and Dore, 2017 (with ~1 resected brain metastasis per patient).

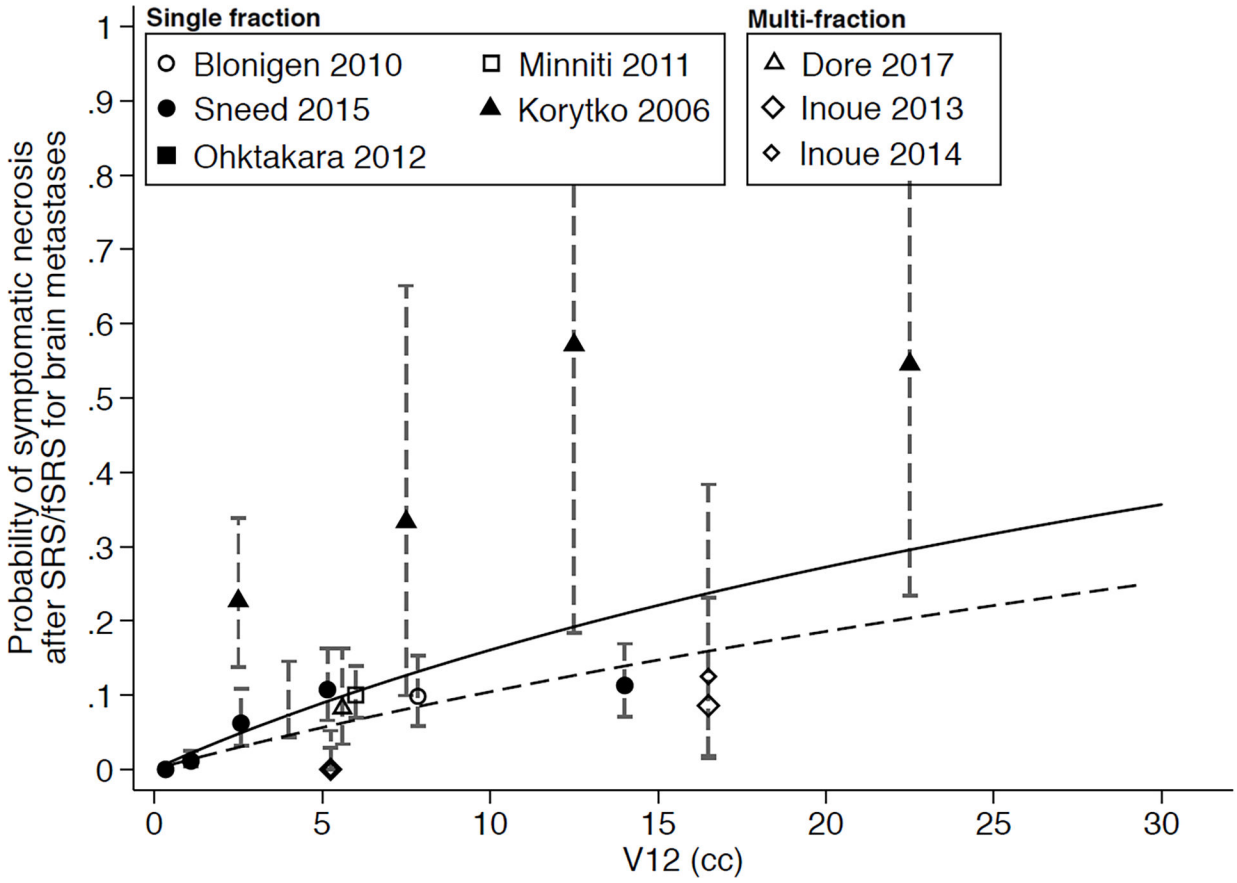

Figure 4.

Risk of symptomatic necrosis after SRS for brain metastases vs. volume of tissue (target plus non-target; solid symbols) or brain (excluding the target volume and non-brain normal tissue; open symbols) receiving ≥12 Gy equivalent in one fraction (V12). All of the studies reported Vx per lesion (see text). Data were extracted from studies that reported necrosis risks and median Vx among all patients/lesions or subgrouped (binned) ranges of Vx and reported the risks of necrosis for patients/lesions within the individual bins. All of the multi-fraction fSRS studies used the endpoint of symptomatic necrosis requiring resection, whereas all of the single-fraction SRS studies used the endpoint of any symptomatic necrosis. The figure represent a rough approximation of data, as (1) the median value of V12 for a given bin was estimated as described in the caption from Figure 1; (2) for multi-fraction SRS studies, the linear-quadratic model with alpha-beta ratio of 2 was used to convert dose to single-fraction equivalent dose; (3) in those studies which reported V10 or V14, the equivalent to V12 was estimated as described in the text (Eq. 2). The error bars represent 95% binomial confidence intervals, and the solid and dashed lines represent fitted logistic models to the single-fraction tissue V12 and multi-fraction brain V12 (in single-fraction equivalent) data, respectively. Single-fraction SRS studies included Korytko, 2006; Blonigen, 2010; Minniti, 2011; Ohtakara, 2012; and Sneed, 2015. Multi-fraction fSRS studies included Inoue, 2013 and 2014, and Dore, 2017 (with ~1 resected brain metastasis per patient); all 3 used brain Vx.

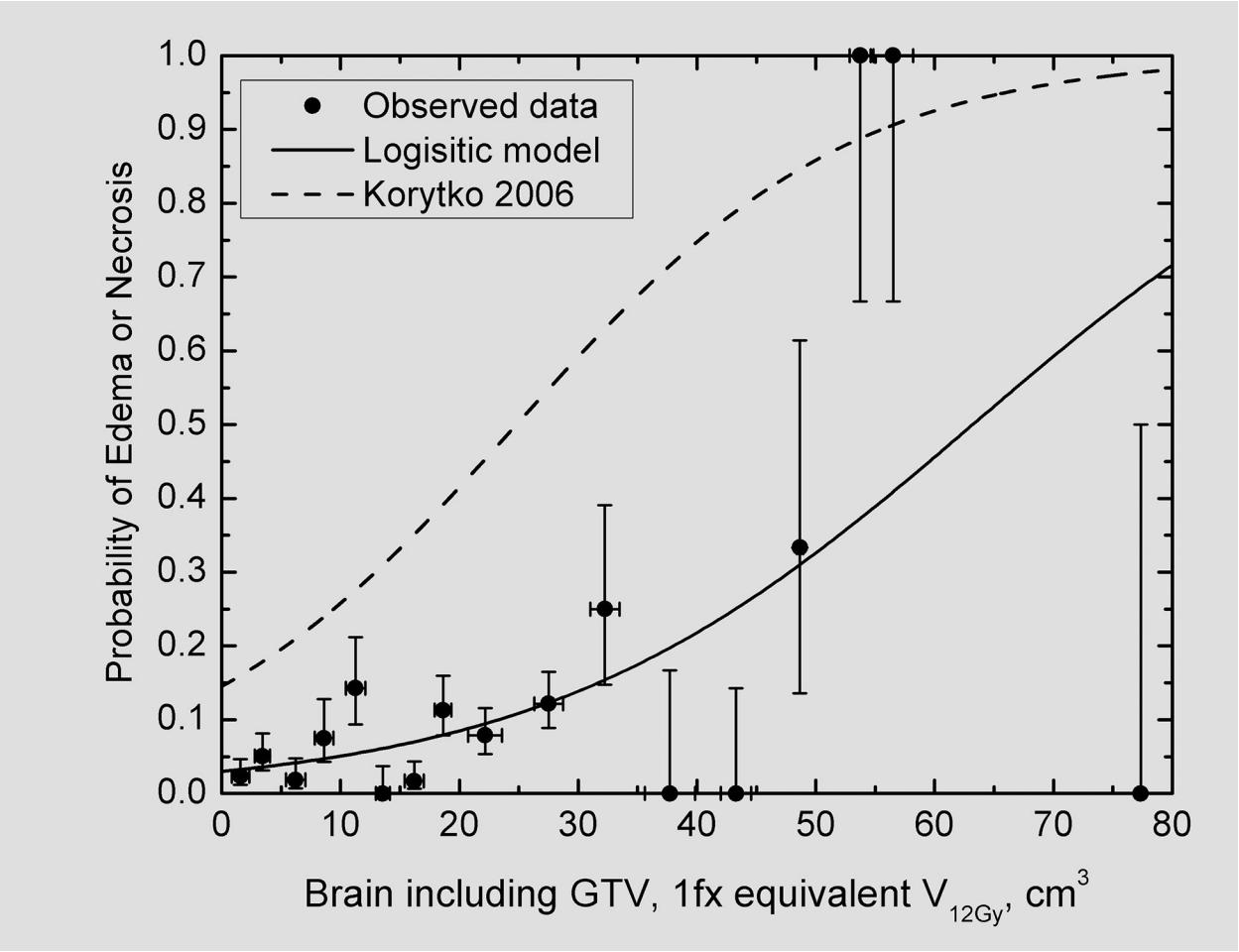

Figure 5.

Aggregate model of edema or necrosis as a function of V12Gy, including GTV, for patients treated with cranial SRS/fSRS, using individual patient data from Chin (2001), Korykto (2006), Inoue (2013), Inoue (2014) and Peng (2018), including 34, 129, 145, 78 and 57 patients (34, 198, 159, 85 and 294 lesions), respectively. Eq. (1) (shown in the text) was used to approximate V12Gy for the aggregated data points from studies by Chin et al., Inoue et al. and Peng et al. The vertical error bars are binomial 68% confidence intervals calculated using the score method and the horizontal error bars are the standard deviations for V12 for a particular bin. Since there were relatively few targets associated with V12Gy >50 cc, the bins in that range tended to quantize towards 0% or 100%. The model parameters for the pooled data are: Vx,50=63.2 (95% CI: 49.2–97.0) and γ50=0.87 (95% CI: 0.74–1.03) with p <0.001 (calculated using chi-squared, based on likelihood ratio by comparing best fit against a horizontal line through incidence averaged over all patients). Because the reported risks from Korytko et al. were substantially greater than in other studies, the unmodified logistic model from their report (dashed line) is shown separately from the others (solid line), and only the other studies are included in the observed data (dots with error bars). The Korytko et al. data points were published in terms of V12Gy.

GTV= gross tumor volume, 1fx= single-fraction equivalent dose using linear quadratic with α/β=2 Gy, V12Gy= the volume of total brain exceeding an equivalent dose of 12 Gy in one fraction. CI= confidence interval.

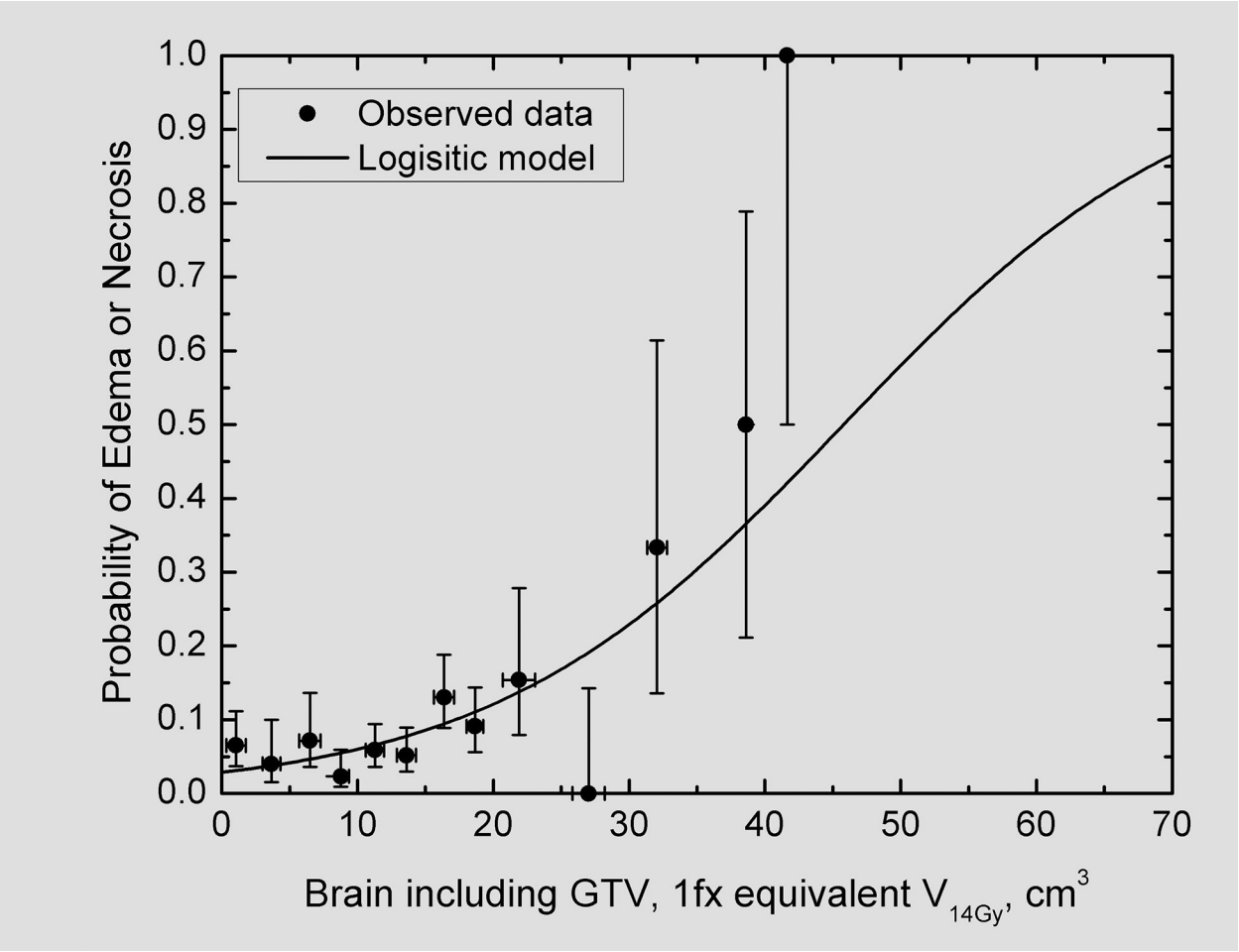

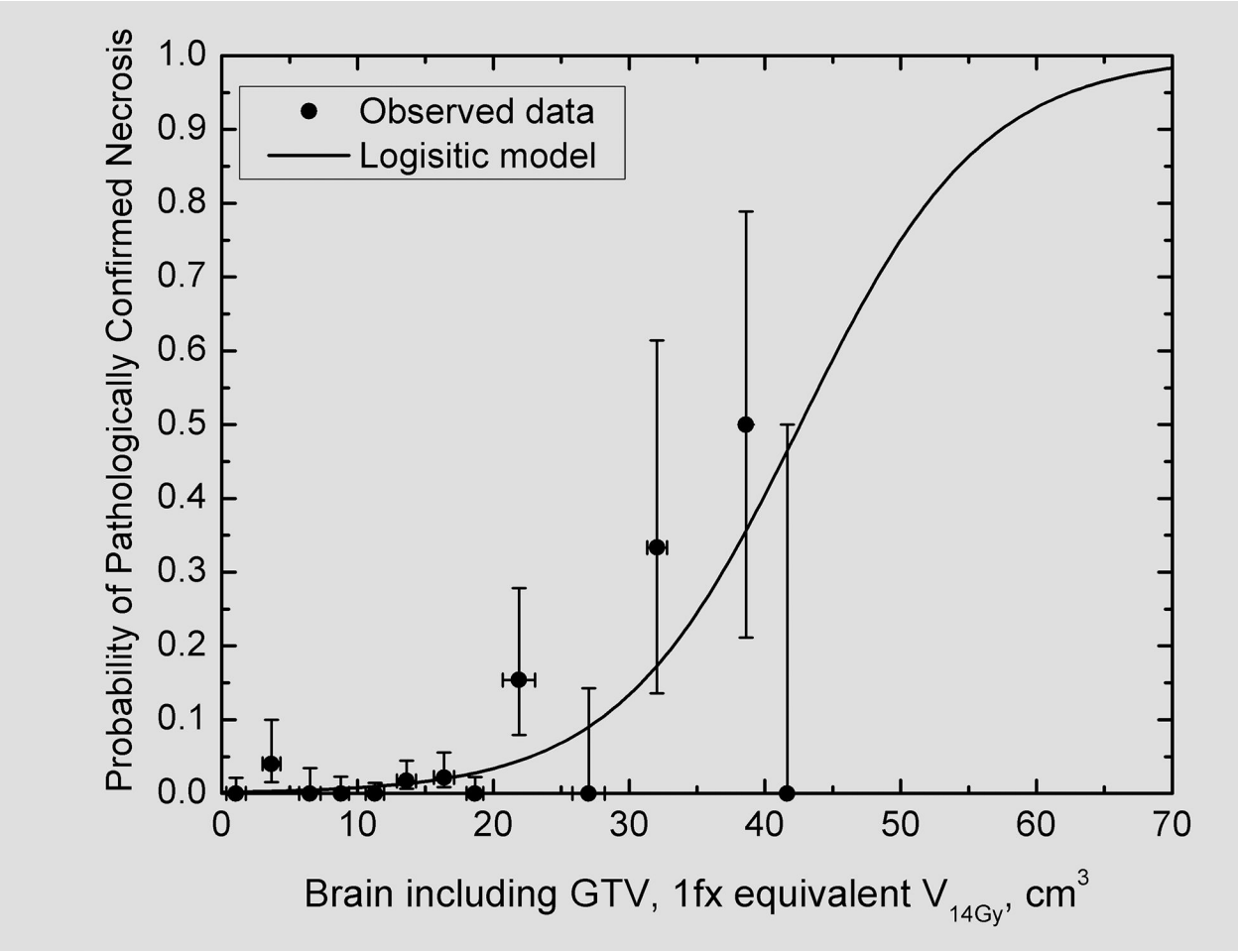

Figure 6.

Volume response normal tissue complication probability models for brain necrosis in patients treated with SRS/fSRS for brain metastases: (A) for grade 1–3 edema or necrosis, and (B) for grade 3 surgically removed and pathologically confirmed necrosis. Data are pooled from 3 studies: Inoue (2013), Inoue (2014) and Peng (2018), including 145, 78 and 57 patients (159, 85 and 294 lesions), respectively. The vertical error bars are binomial 68% confidence intervals calculated using the score method and the horizontal error bars are the standard deviations for V14 for a particular bin. The model parameters for the pooled data are: for Figure 6A, Vx,50=45.8 (95% CI: 33.0–106.2) and $\gamma 50=0.88$ (95% CI: 0.68–1.11) with p=0.003; for Figure 6B, Vx,50=42.6 (95% CI: 33.8–75.5) and $\gamma 50=1.58$ (95% CI: 1.17–2.09) with p<0.001. p values were calculated using chi-squared, based on likelihood ratio by comparing best fit against a horizontal line through incidence averaged over all patients. GTV= gross tumor volume, 1fx= single-fraction equivalent dose using linear quadratic with $\alpha/\beta=2$ Gy, V14Gy= the volume of total brain exceeding an equivalent dose of 14 Gy in one fraction. CI=confidence interval

Table 1:

Scoring systems for brain toxicity (not specific to necrosis).

RTOG/EORTC acute morbidity score (from 1995)	
Grade 0	None
Grade 1	Fully functional status (i.e. able to work) with minor neurologic findings. No medication needed
Grade 2	Neurological findings present sufficient to require home care/ nursing assistance may be required/medications including steroids/antiseizure agents may be required
Grade 3	Neurological findings requiring hospitalization for initial management
Grade 4	Serious neurological impairment that includes paralysis, coma, or seizures >3 per week despite medication/ hospitalization required
CTCAE version 4 (from 2009)	
Grade 0	None
Grade 1	Asymptomatic; clinical or diagnostic observations only; intervention not indicated
Grade 2	Moderate symptoms; corticosteroids indicated
Grade 3	Severe symptoms; medical intervention indicated
Grade 4	Life-threatening consequences; urgent intervention indicated

Abbreviations: RTOG: Radiation Therapy Oncology Group; EORTC: European Organization for Research and Treatment of Cancer

Table 2:

Studies included in the dose-response models for NTCP of brain necrosis following SRS for brain metastases

Author (Year)	Num. fractions	SRS System	Vx	Definition of Analyzed Brain	Tumor types	# targets / # patients (ratio)	Endpoint
Chin (2001)	1	GK	V10Gy	Total 10 Gy volume	mixed	NR / 233	Pathological confirmation on MR imaging of radiation necrosis, or development of a necrotic lesion that resolved over time
Korytko (2006)	1	GK	V12Gy	Total 12 Gy volume	mixed	**198** / 127 (1.56)	Symptomatic radiation necrosis
Inoue (2013)	3	CK	V14Gy SFED	14 Gy volume excluding GTV	BM	**159** / 145 (1.10)	Datapoints 1: G1–3 edema and necrosis, Datapoints 2: G3 pathologically confirmed
Inoue (2014)	5	CK	V14Gy SFED	14 Gy volume excluding GTV	BM	**85** / 79 (1.09)	Datapoints 1: G1–3 edema and necrosis, Datapoints 2: G3 pathologically confirmed
Peng (2018)	1, 3, 5 *	CK	V14Gy SFED	Brain 14 Gy Volume (target not subtracted)	BM	294 / **139** *(2.12)	Model 1: G1–3 edema and necrosis, and Model 2: G3 pathologically confirmed

G=grade; GTV=gross target volume; SFED=single fraction equivalent dose calculated using the linear quadratic model with α/β=2 Gy. Mixed = brain metastases, glioma and benign brain tumors (see Supplemental Table 1 for specific details)

*n= 96, 23 and 20 treatment with 1, 3 and 5 fractions respectively. 57 patients with 139 treatment plans.

Int J Radiat Oncol Biol Phys. Author manuscript; available in PMC 2022 August 18.

Table 3:

Estimated risk, from dose-response models for NTCP, of brain radionecrosis following SRS for brain metastases at various dose/volume levels

Vx metric (x in Gy)			Toxicity grade	Toxicity rate for Vx ≥			Studies in NTCP model
1-fraction	3-fractions†	5-fractions†		5 cc	10 cc	20 cc	
V12	V19.6	V24.4	1–3	3.6%	4.8%	8.6%	Chin, 2001* + Inoue, 2013 + Inoue, 2014 + Peng, 2018
V12	V19.6	V24.4	1–3	19.6%	25.8%	41.5%	Korytko, 2006*
V14	V23.1	V28.8	1–3	4.1%	6.0%	12.1%	Inoue, 2013 + Inoue, 2014 + Peng, 2018
V14	V23.1	V28.8	3	0.4%	0.8%	3.4%	Inoue, 2013 + Inoue, 2014 + Peng, 2018

*These studies included patients with brain metastases as well as other intracranial tumors (see Supplemental Table 1 for specific details)

†Equivalent doses are calculated with the linear quadratic model and $\alpha/\beta=2$ Gy.